Renormalization group improved determination of light quark masses from Borel-Laplace sum rules

M. S. A. Alam Khan⊙*

Centre for High Energy Physics, Indian Institute of Science, Bangalore 560 012, India

We determine masses of light quarks (m_u, m_d, m_s) using Borel-Laplace sum rules and renormalization group summed perturbation theory (RGSPT) from the divergence of the axial vector current. The RGSPT significantly reduces the scale dependence of the finite-order perturbative series for the renormalization group invariant quantities such as spectral function, the second derivative of the polarization function of the pseudoscalar current correlator, and its Borel transformation. In addition, the convergence of the spectral function is significantly improved by summing all running logarithms and kinematical π^2-terms. Using RGSPT, we find $m_s(2 \text{ GeV}) = 104.34^{+4.32}_{-4.21}$ MeV and $m_d(2 \text{ GeV}) = 4.21^{+0.48}_{-0.45}$ MeV leading to $m_u(2 \text{ GeV}) = 2.00^{+0.33}_{-0.38}$ MeV.

I. INTRODUCTION

The light quark masses are important parameters for quantum chromodynamics (QCD) and electroweak physics. Because of confinement, they are not freely observed, and their values depend on the scheme used. They are taken as input in various quantities related to flavor physics and play a key role in the proton-neutron mass difference and the strong CP violating observable ϵ'/ϵ, etc. Precise determination of their values has been of constant interest in the past three decades. These masses can be precisely obtained using the lattice QCD simulations, and for recent development, we refer to Ref. [1].

Theoretical tools such as the QCD sum rules [2,3] have played a key role in their precise determination. These sum rules use both theoretical and experimental input on the spectral function and are based on the assumption of the quark-hadron duality [4]. On the hadronic side, the spectral functions for the pseudoscalar channel in the case of the strange and nonstrange channels do not have experimental data, and therefore, inputs from chiral perturbation theory (ChPT) [5–7] become very important. For reviews, we refer to [8–10] and references therein.

On the theoretical side, operator product expansion (OPE) [11] is used, which has perturbative and nonperturbative contributions. The perturbative corrections are calculated by

*alam.khan1909@gmail.com

evaluating the Feynman diagrams, and nonperturbative corrections are the condensates of higher-dimensional operators of quarks and gluons fields. The condensates can be determined from lattice QCD, ChPT, or using QCD sum rules [12].

Fixed-order perturbation theory (FOPT) is the most commonly used prescription in the literature. In this prescription, the perturbative series is a polynomial in the strong coupling constant $[\alpha_s(\mu)]$, quark masses $[m_q(\mu)]$, and the running renormalization group (RG) logarithms $[\log(\mu^2/Q^2)]$. The RG invariance of an observable $(\mathcal{O})$, known to a finite order in perturbation theory, is enforced using the RG equation (RGE),

$$\mu^2 \frac{d}{d\mu^2} \mathcal{O} = 0, \tag{1}$$

which results in a cancellation among the coefficients of different orders in α_s. The solution to Eq. (1) can be used to generate the RG logarithms.

Renormalization group summed perturbation theory (RGSPT) is a perturbative prescription in which the running RG logarithms arising from a given order of the perturbation theory are summed in a closed form to all orders using RGE. As a result, we get an analytical expression for the perturbative series in which $\alpha_s(\mu) \log(\mu^2/Q^2) \sim \mathcal{O}(1)$. This scheme is useful in reducing the theoretical uncertainties arising from renormalization scale dependence. The procedure is described in Sec. III and some of the applications can be found in Refs. [13–26].

The Borel-Laplace sum rule is one of the important methods widely used in the literature, especially for the determinations of quark mass [27–35] and in the extraction

of hadronic parameters [36–39], etc. However, the dependence of an unphysical Borel parameter (u) and free continuum threshold s_0 parameter is present in these determinations. In principle, any determination using this sum rule should be independent of the choice of these parameters, but they are tuned to get reliable results. In addition, the determination of the light quark masses from these sum rules is found to be very sensitive to the renormalization scale, and a linear behavior has been reported in Refs. [28,40]. Also, suppression to the hadronic spectral function using pinched kernels [27,41], mainly used in the finite energy sum rules (FESR), cannot be implemented in these sum rules.

With the limitations in hand, our interest in this sum rule is because of two reasons:

(1) The formalism developed in Ref. [23] can be used to improve the convergence and reduced renormalization scale dependence for the spectral function by summing kinematical π^2-terms using RGSPT.

(2) All-order summation of the Euler's constant (γ_E) and ζ functions arising as a result of the Borel transformation of the RG invariant second derivative of the polarization function using RGSPT.

It should be noted that these improvements are very crucial and can be used in any Borel-Laplace sum-rule-based studies. On the theoretical side, the leading perturbative $\mathcal{O}(\alpha_s^4)$ corrections to the pseudoscalar two-point function are now available in Refs. [42–44] and other OPE corrections from Refs. [28,35,45–47]. For the low-energy region, there is no experimental information for the pseudoscalar spectral density in the resonance region, but it can be modeled using the experimental values of the resonances [48–50]. We have used the results of previous studies on the hadronic spectral function from Refs. [29,48–51] for the strange and nonstrange channel.

Hadronic τ decays are also found to be very useful in the determination of strange quark mass, Cabibbo-Kobayashi-Maskawa element $|V_{us}|$, and strong coupling constant, and more details can be found in Refs. [15,52–57]. These studies use experimental data on the spectral function. Commonly used prescriptions for the perturbative series in these FESR-based studies use FOPT and contour improved perturbation theory (CIPT). Recently, CIPT has been found to be in conflict with the OPE expectations, and for more details, we refer to Refs. [58–64]. For other light quark mass determinations using sum rules, we refer to Refs. [34,40,48,65].

It should be noted that only the $\overline{\text{MS}}$ definition of α_s and m_q is used in this article. The value of $\alpha_s(M_z) = 0.1179 \pm 0.0009$ has been taken from the PDG [66] and evolved to different scales using the five-loop β function for three flavors using packages REvolver [67] and RunDec [68,69]. Its value at τ lepton mass (M_τ) scale is $\alpha_s(M_\tau) = 0.3139 \pm 0.0083$ and has been used in this article. Also, we have used couplant $x(\mu) \equiv \frac{\alpha_s(\mu)}{\pi}$ as an expansion parameter in the

perturbation series and if explicit energy scale is not shown, then x are assumed to be evaluated at renormalization scale μ.

In Sec. II, we briefly introduce the quantities needed for the Borel-Laplace sum rule. In Sec. III, we give a short review of RGSPT. In Sec. IV, hadronic parametrization of the spectral function for the strange and nonstrange channel is discussed. In Sec. V, OPE contribution and its results in FOPT and RGSPT prescription are discussed. In Sec. VI, results from the previous sections are used for the light quark mass determinations. In Sec. VII, we give the summary and conclusion of this article, and supplementary information is provided in Appendixes A and B.

II. FORMALISM

The current correlator for the divergence of the axial currents is defined as

$$\Psi_5(q^2) \equiv i \int d^4x e^{iqx} \langle 0|\mathcal{T}\{j_5(x)j_5^\dagger(0)\}|0\rangle, \quad (2)$$

where j_5 is given by

$$\begin{aligned} j_5 &= \partial^\mu(\bar{q}_1\gamma_\mu\gamma_5 q_2) = i(m_1 + m_2)(\bar{q}_1\gamma_5 q_2) \\ &= i(m_1 + m_2)j_0, \end{aligned} \quad (3)$$

and quark masses m_i as well as quark fields $q_i \equiv q_i(x)$ are bare quantities.

Using Eq. (3), the correlation function in Eq. (2) after renormalization in the $\overline{\text{MS}}$ scheme is related to the pseudoscalar polarization function [$\Pi_P(q^2, \mu^2)$] by relation

$$\Psi_5(q^2) = (m_1 + m_2)^2 \Pi_P(q^2, \mu^2), \quad (4)$$

where $m_i \equiv m_i(\mu)$. The polarization function $\Pi_P(q^2, \mu^2)$ is given by

$$\Pi_P(q^2, \mu^2) = i \int d^4x e^{iqx} \langle 0|\mathcal{T}\{j_0(x)j_0^\dagger(0)\}|0\rangle, \quad (5)$$

where j_0 is a renormalized current in the $\overline{\text{MS}}$ scheme. Because of the above relation, the sum rule determinations from the correlator in Eq. (2) are sometimes known as pseudoscalar determinations.

Using OPE, a theoretical expression for $\Psi_5(q^2)$ is calculated in the deep Euclidean spacelike regions in the limit $m_q^2 \ll q^2$, and the resulting expansion can be arranged as expansion in $1/(q^2)$. At low energies ~ 1 GeV^2, instanton effects become relevant, and their contribution is not captured by OPE and therefore are added to it. Further details on the OPE contributions are presented in Sec. V.

The Borel-Laplace sum rules are based on the double-subtracted dispersion relation for the correlation function. Therefore, it involves the double derivative of $\Psi_5(q^2)$ and the dispersion relation is given by

$$\Psi_5''(q^2) = \frac{d^2}{d(q^2)^2}\Psi_5(q^2) = \frac{2}{\pi}\int_0^\infty ds \frac{\mathrm{Im}\Psi_5(-s-i\epsilon)}{(s-q^2-i\epsilon)^3}. \quad (6)$$

The Borel transformation,[1] with parameter "u," is obtained using the Borel operator $\hat{\mathcal{B}}_u$, defined as

$$\hat{B}_u \equiv \lim_{\substack{Q^2,n\to\infty \\ Q^2/n=u}} \frac{(-Q^2)^n}{\Gamma[n]}\partial_{Q^2}^n, \quad (7)$$

where we have used variables $Q^2 = -q^2 > 0$ for the spacelike and $s = q^2 > 0$ for timelike regions.

Borel parameter u has the dimension of GeV^2 and the Borel transform of Eq. (6) is obtained as

$$\begin{aligned}\Psi_5''(u) &\equiv \hat{B}_u[\Psi_5''(q^2)] = \frac{1}{u^3}\hat{B}_u[\Psi_5(q^2)](u)\\ &= \frac{1}{\pi u^3}\int_0^\infty ds\, e^{-s/u}\mathrm{Im}\Psi_5(-s-i\epsilon)\\ &= \frac{1}{u^3}\int_0^\infty ds\, e^{-s/u}\rho_5(s),\end{aligned} \quad (8)$$

where the spectral density is given by

$$\rho_5(s) = \frac{1}{\pi}\lim_{\epsilon\to 0}[\mathrm{Im}\Psi_5(-s-i\epsilon)]. \quad (9)$$

It should be noted that the value of the $u \gg \Lambda_{\mathrm{QCD}}^2$ in $\Psi_5''(u)$ is chosen such that higher-order terms of the OPE remain suppressed in the Borel transformed OPE.

The Borel-Laplace sum rules on the rhs of Eq. (8) involve an integration ranging from the low-energy regime of the strong interactions to the high-energy regime. The spectral density is approximated with the quark-hadron duality. For the low-energy regime, the spectral function is parametrized in terms of pion/kaon poles and resonances present in the channel, and for the high-energy region, results from perturbative QCD (pQCD) are used. The spectral density from these two regimes can be written as

$$\rho_5(s) = \theta(s_0 - s)\rho_5^{\mathrm{had}}(s) + \theta(s - s_0)\rho_5^{\mathrm{OPE}}(s), \quad (10)$$

where scale s_0 separates the two contributions, and its value should be chosen such that the perturbative treatment is justified.

Using Eq. (10), the Borel sum rule in Eq. (8) can be written as

---

[1]We use normalization given in Ref. [35], i.e., $\hat{\mathcal{B}}_u[\frac{1}{(x+s)^a}] = \frac{1}{u^a\Gamma[a]}e^{-x/u}$.

$$\begin{aligned}\Psi_5''(u) &= \frac{1}{u^3}\int_0^{s_0} ds\, e^{-s/u}\rho_5^{\mathrm{had}}(s)\\ &+ \frac{1}{u^3}\int_{s_0}^\infty ds\, e^{-s/u}\rho_5^{\mathrm{OPE}}(s),\end{aligned} \quad (11)$$

which is used in this article for the light quark mass determination.

For clarification, various inputs used in Eq. (11) are as follows:

(1) The $\Psi_5''(u)$ is obtained from the Borel transformation of $\Psi''(q^2)$, which involves OPE corrections and addition to the instanton contributions. The instanton contributions are small for the choice of the parameters used in this article, but relevant as pointed out in Ref. [48]. These contributions are thus obtained using Eqs. (43) and (68).

(2) The hadronic spectral density $\rho_5^{\mathrm{had}}(s)$ is obtained by the parametrization of the experimental information on the hadrons appearing in the strange and nonstrange channels. These constitutions are discussed in Sec. IV for nonstrange and strange channels, and we use Eq. (22) or (25).

(3) $\rho_5^{\mathrm{OPE}}(s)$ on the rhs of Eq. (11) is obtained from the discontinuity of the theoretical expression of the $\Psi_5(q^2)$ which is calculated using the OPE and instanton contributions are also added to it. It has contributions from Eqs. (44) and (67).

(4) Quark mass appears on both sides of Eq. (11) except for the integral term containing $\rho_5^{\mathrm{had}}(s)$.

It should be noted that the main focus of this article is the RG improvement for the theoretical quantities relevant for points 1 and 3 and its impact in the light quark mass determination.

III. REVIEW OF THE RGSPT

In FOPT prescription, a perturbative series $\mathcal{S}(Q^2,\mu^2)$ in pQCD can be written as

$$\mathcal{S}(Q^2,\mu^2) \equiv \sum_{i=0,j=0}^{j\leq i} T_{i,j}x^i L^j, \quad (12)$$

where $x = \alpha_s(\mu)/\pi$ and $L = \log(\mu^2/Q^2)$. The RG evolution of the perturbative series in Eq. (12) is obtained using its anomalous dimension $\gamma_S(x)$ by solving

$$\mu^2\frac{d}{d\mu^2}\mathcal{S}(Q^2,\mu^2) = \gamma_S(x)\mathcal{S}(Q^2,\mu^2), \quad (13\mathrm{a})$$

$$\mu^2\frac{d}{d\mu^2}x(\mu) = \beta(x), \quad (13\mathrm{b})$$

where anomalous dimension $\gamma_S(x)$ and $\beta(x)$ are given by

$$\gamma_S(x) = \sum_{i=0}\gamma_i x^{i+1}, \qquad \beta(x) = \sum_{i=0}\beta_i x^{i+2}. \quad (14)$$

The perturbative series in Eq. (12) has no large logarithms if we set $\mu^2 = Q^2$ and various parameters, such as quark masses and couplings, are evolved to different scales using their RG equations. To account for renormalization scale dependence for a series with vanishing anomalous dimension, we set $\mu^2 = \xi Q^2$ and the parameter ξ is often varied in the range $\xi \in [1/2, 2]$. The RG logarithms in Eq. (12) still play a key role in canceling the scale dependence arising from other parameters, such as from α_s and m_q.

In RGSPT, perturbative series in Eq. (12) is arranged as follows:

$$\mathcal{S}^\Sigma(Q^2, \mu^2) = \sum_i x^i S_i(xL), \qquad (15)$$

where the goal is to obtain a closed-form expression for coefficients

$$S_i(z) = \sum_{j=0}^{\infty} T_{i+j,j} z^j, \qquad (16)$$

where $z \equiv xL$. $S_i(z)$ are functions of one variable where $z \sim \mathcal{O}(1)$. The closed-form solution for them is obtained using RGE.

The RGE in Eq. (13a) results in a set of coupled differential equations for $S_i(z)$, which in compact form can be written as

$$\left(\sum_{i=0}^{n} \frac{\beta_i}{z^{n-i-1}} \frac{d}{dz} (z^{n-i} S_{n-i}(z)) + \gamma_i S_{n-i}(z) \right) - S_n'(z) = 0, \qquad (17)$$

The first three coefficients can be obtained by solving the above differential equation and are given by

$$
\begin{aligned}
S_0(z) &= T_{0,0} w^{-\tilde{\gamma}_0}, \\
S_1(z) &= T_{1,0} w^{-\tilde{\gamma}_0 - 1} + T_{0,0} w^{-\tilde{\gamma}_0 - 1} [(1-w)\tilde{\gamma}_1 + \tilde{\beta}_1 \tilde{\gamma}_0 (w - \log(w) - 1)], \\
S_2(z) &= T_{2,0} w^{-\tilde{\gamma}_0 - 2} - T_{1,0} w^{-\tilde{\gamma}_0 - 2} [(w-1)\tilde{\gamma}_1 + \tilde{\beta}_1 (\tilde{\gamma}_0 (-w + \log(w) + 1) + \log(w))] \\
&\quad + \frac{1}{2} T_{0,0} w^{-\tilde{\gamma}_0 - 2} \{ -\tilde{\beta}_1 \tilde{\gamma}_1 [1 - w^2 + 2\log(w) + 2(w-1)\tilde{\gamma}_0 (w - \log(w) - 1)] \\
&\quad + (w-1)[(w-1)\tilde{\beta}_2 \tilde{\gamma}_0 + (w-1)\tilde{\gamma}_1^2 - (w+1)\tilde{\gamma}_2] + \tilde{\beta}_1^2 \tilde{\gamma}_0 (\tilde{\gamma}_0 - 1)(w - \log(w) - 1)^2 \},
\end{aligned}
\qquad (18)
$$

where $w \equiv 1 - \beta_0 z$, and for anomalous dimension and higher-order beta function coefficients, we have used $\tilde{X} \equiv X/\beta_0$. The important feature of the above procedure is that the most general term of RGSPT is given by

$$\Omega_{n,a} \equiv \frac{\log^n(w)}{w^a} = \frac{\log^n(1 - \beta_0 x(\mu) \log(\mu^2/Q^2))}{(1 - \beta_0 x(\mu) \log(\mu^2/Q^2))^a}, \quad (19)$$

where n is a positive integer and $a \propto \gamma_0/\beta_0$ appearing in Eq. (14). It should be noted that, for $\mu^2 = Q^2$, both RG summed series in Eqs. (15) and (12) agree with each other. The analytic continuation for them is obtained by taking discontinuity of $\log(\mu^2/Q^2) = \log(\mu^2/|Q|^2) \pm i\pi$. This procedure results in large "$i\pi$" corrections for FOPT, but for RGSPT, such corrections are summed to all orders in the terms like in Eq. (19). For numerical prescriptions such as CIPT, the analytic continuation is obtained by using Eq. (46). One important point to note here is that results from different prescriptions, such as RGSPT and FOPT, are not the same when $\mu^2 = Q^2$ is set after operations like analytic continuation or Borel transformation are performed. The differences arise due to different treatments of the RG logarithms for finite-order series for which only a few terms are known. For more details on analytic continuation using FOPT and RGSPT, we refer to Ref. [23].

The reduced sensitivity on the renormalization scale in RGSPT prescription is due to the cancellation between running parameters [coupling and masses by numerically solving Eqs. (13a) and (13b)] and coefficients $S_i(z)$ at different orders. For a simpler case, in which series Eq. (12) with vanishing anomalous dimension [$\gamma_i = 0$ in Eq. (18)], there is a perfect cancellation between $S_1(z)$ in Eq. (18) and exact one-loop running of the strong coupling constant $[x(\sqrt{\xi}\mu) = \frac{x(Q)}{1 - x(Q)\beta_0 \log(Q^2/(\xi\mu^2))} + \mathcal{O}(x^2)]$. It is not easier to such perfect cancellation for higher orders, as the exact analytical solution to x, using Eq. (13b), is not known.

An alternate way to achieve RG improvement and access would be to rearrange the original series in Eq. (12) by replacing running logarithms as

$$\log\left(\frac{\mu^2}{Q^2} \right) = -\log(\xi) + \log\left(\xi \frac{\mu^2}{Q^2} \right) = -\log(\xi) + L_\xi, \quad (20)$$

and get a closed-form summation, similar to Eq. (15), that has the form

$$\mathcal{S}^{\Sigma_\xi} = \sum_i x(\mu)^i S_i(\xi, x(\mu) L_\xi). \qquad (21)$$
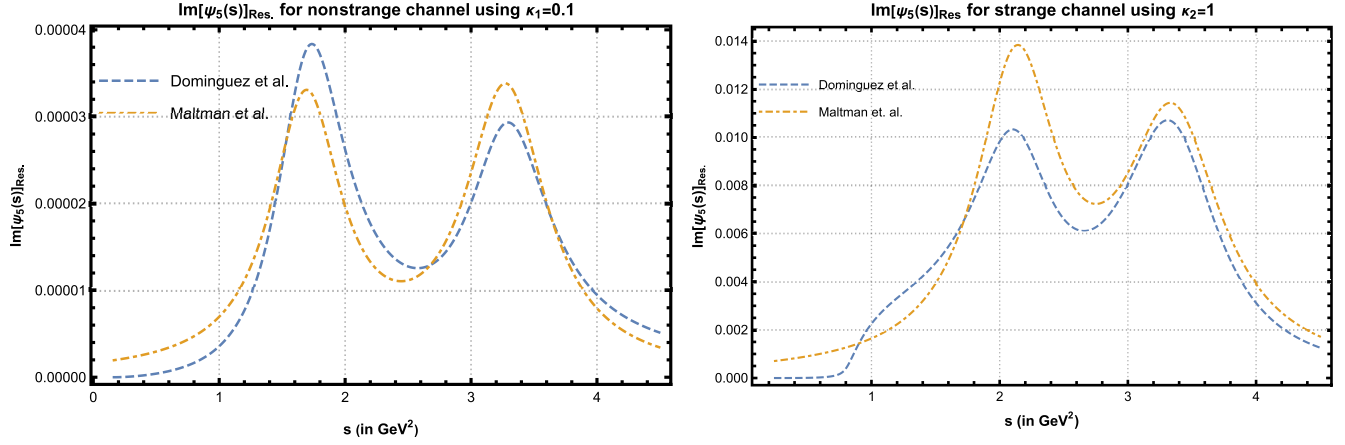
FIG. 1. Hadronic spectral function in the resonance region for strange and nonstrange channels using Dominguez and de Rafael's parametrization [49].

Such a summation is not performed for RGSPT in the literature and is left for future studies.[2]

IV. HADRONIC SPECTRAL FUNCTION

The hadronic spectral functions are constructed using the contributions from the pion/kaon pole and the data from the experiments on the resonances in a given channel. At low energies, they are dominated by the pion/kaon pole contributions. This section discusses the parametrization of the unknown pseudoscalar spectral function for the nonstrange and strange channels.

A. Nonstrange channel

For the nonstrange pseudoscalar channel, two phenomenological parametrizations are often used in the literature. In Ref. [49], Dominguez and de Rafael provided a ChPT-based parametrization that is normalized to unity at the threshold. Later, some corrections are reported for this parametrization in Ref. [50]. Another parametrization often used is by Maltman and Kambor [48], which requires masses and decay constants for the higher resonances. In this article, we have used Dominguez and de Rafael's parametrization, which was recently used in Ref. [65] for the up/down-quark mass determination. We have used their results for the nonstrange spectral function (ρ_{NS}) and the hadronic parametrization is given by:

$$\rho_{NS} = f_\pi^2 M_\pi^4 \delta(s - M_\pi^2) + \rho_{3\pi} \frac{BW_1(s) + \kappa_1 BW_2(s)}{1 + \kappa_1}, \quad (22)$$

where f_π and M_π are the decay constant and mass of the pion. The value of $\kappa_1 \simeq 0.1$ is used in the Ref. [65] and it controls the relative importance of the resonances. The 3π resonance contributions are received from the $\pi(1300)$ and $\pi(1800)$ states. Their contributions are encoded in the $\rho_{3\pi}$, which is given by

$$\rho_{3\pi} = \frac{1}{\pi} \mathrm{Im}\Psi_5(s)\Big|_{3\pi} = \frac{1}{9} \frac{M_\pi^2}{f_\pi^2} \frac{1}{2^7 \pi^4} \theta(s - 9M_\pi^2) I_\pi(s), \quad (23)$$

where $I_\pi(s)$ is the phase space integral given in Eq. (29). In the chiral limit, the phase integral reduces to $I_\pi(s) = 3s$ that confirms the prediction for $\rho_{3\pi}$ in Ref. [70]. The $BW_{1,2}(s)$ is the Breit-Wigner distribution given by

$$BW_i(s) = \frac{(M_i^2 - s_{th})^2 + M_i^2 \Gamma_i^2}{(s - M_i^2)^2 + M_i^2 \Gamma_i^2}, \quad (24)$$

which is normalized to unity at the threshold, i.e., $BW_{1,2}(s_{th}) = 1$. For the nonstrange spectral function, we use the following data from the PDG [66] as input:

$$M_\pi = 134.9768(5), \qquad f_\pi = 130.2(1.2) \text{ MeV},$$
$$M_{\pi,1} = 1300(100), \qquad \Gamma_{\pi,1} = 260(36) \text{ MeV},$$
$$M_{\pi,2} = 1810^{+11}_{-9}, \qquad \Gamma_{\pi,2} = 215^{+7}_{-8} \text{ MeV}.$$

Using the above values as input, the nonstrange spectral function in the two parametrizations discussed above is plotted in Fig. 1.

B. The strange channel

We use the hadronic parametrization presented in Ref. [29] for the strange channel. This parametrization is equivalent to the one we have used in the nonstrange channel. The hadronic spectral function is given by

$$\rho_S(s) = \frac{1}{\pi} \mathrm{Im}\Psi_5(s)\Big|_{\text{Had.}}$$
$$= f_K^2 M_K^2 \delta(s - M_K^2) + \frac{1}{\pi} \mathrm{Im}(\Psi_5(s))\Big|_{\text{Res.}}, \quad (25)$$

where the spectral function for the resonance region is given by

---

[2]We thank the referee for pointing out this alternate method to explore the scale dependence in RGSPT.

$$\frac{1}{\pi}\text{Im}(\Psi_5(s))\Big|_{\text{Res.}} = \rho_{K\pi\pi}(s)\frac{\text{BW}_1(s) + \kappa_2\text{BW}_2(s)}{1 + \kappa_2}. \quad (26)$$

The Breit-Wigner profile is constructed from $K(1460)$ and $K(1830)$ resonances. The value $\kappa_2 \simeq 1$ is found to be a reasonable choice in Ref. [29] to control the contributions from the resonances. In addition, due to its narrow width, there is a significant contribution from the resonant sub-channel $K^*(892) - \pi$. Its contributions are also included in the $\rho_{K\pi\pi}(s)$ and has the form:

$$\rho_{K\pi\pi}(s) = \frac{M_K^2}{2f_\pi^2}\frac{3}{2^7\pi^4}\theta(s - M_K^2)\frac{I_K(s)}{s(M_K^2 - s)}, \quad (27)$$

and the integral $I_K(s)$ is defined in Eq. (31). For the strange channel, precise values of the resonance masses and the

decay width do not exist. We are using the values used in Ref. [51] with additional uncertainties of 50 MeV to resonance masses and 10% to the decay widths. For kaons, we use PDG [66] values, and the following values for the parameters for the strange channel are used as input:

$$M_K = 497.611(13), \qquad f_K = 155.7(3) \text{ MeV},$$
$$M_{K,1} = 1460(50), \qquad \Gamma_1 = 260(26) \text{ MeV},$$
$$M_{K,2} = 1830(50), \qquad \Gamma_1 = 250(25) \text{ MeV},$$
$$M_{K^*} = 895.55(2), \qquad \Gamma_{K^*} = 47.3(5) \text{ MeV}. \quad (28)$$

Using the above inputs, the strange spectral function in the resonance region is plotted in Fig. 1,

$$I_\pi(s) = \int_{4M_\pi^2}^{(\sqrt{s}-M_\pi)^2} du\sqrt{1 - \frac{4M_\pi^2}{u}}\frac{\lambda^{1/2}(s, u, M_\pi^2)}{s}\left\{5 + \frac{1}{(s - M_\pi^2)}[3(u - M_\pi^2) - s + 9M_\pi^2]\right.$$
$$\left. + \frac{1}{2(s - 4M_\pi^2)^2}\left[(s - 3u + 3M_\pi^2)^2 + 3\lambda(s, u, M_\pi^2)\left(1 - 4\frac{M_\pi^2}{u}\right) + 20M_\pi^4\right]\right\}, \quad (29)$$

where $\lambda(s, u, M_\pi^2)$ is given by

$$\lambda(s, u, M_\pi^2) = (s - (\sqrt{u} - M_\pi)^2)(s - (\sqrt{u} + M_\pi)^2), \quad (30)$$

$$I_K(s) = \int_{M_K^2}^s \frac{du}{u}(u - M_K^2)(s - u)\left\{(M_K^2 - s)\left[u - \frac{(s + M_K^2)}{2}\right] - \frac{1}{8u}(u^2 - M_K^4)(s - u) + \frac{3}{4}(u - M_K^2)^2|F_{K^*}(u)|^2\right\}, \quad (31)$$

and

$$|F_{K^*}(u)|^2 = \frac{(M_{K^*}^2 - M_K^2)^2 + M_{K^*}^2\Gamma_{K^*}^2}{(M_{K^*}^2 - u)^2 + M_{K^*}^2\Gamma_{K^*}^2}. \quad (32)$$

V. THE OPE CORRECTIONS

The OPE corrections are calculated in large Q^2 limit and organized as expansion in $1/Q^2$,

$$\Psi_5(Q^2) = Q^2(m_1 + m_2)^2\sum_{i=0}\frac{\Psi_{2i}(Q^2)}{(Q^2)^i}, \quad (33)$$

and $\Psi_{2n}(Q^2)$ are termed as the contributions from $2n$-dimensional operators for $n = 0, 1, 2, 3, \ldots$. Quantities $\Psi_0(Q^2)$ and $\Psi_2(Q^2)$ are purely perturbative, while additional nonperturbative condensate corrections start from $\Psi_4(Q^2)$. The leading term in the OPE, $\Psi_0(Q^2)$, is known to $\mathcal{O}(\alpha_s^4)$ [42–44], which has an expansion in terms of α_s and $\log(\mu^2/Q^2)$. The dimension-two term of OPE, $\Psi_2(Q^2)$, receives massive corrections ($\propto m_i^2$) and it is known to $\mathcal{O}(\alpha_s^1)$ [35,45–47]. Additional strange quark mass

corrections $[\propto \mathcal{O}(m_s^2\alpha_s^2)]$ to it are included from Ref. [28]. The nonlogarithmic terms appearing in $\Psi_0(Q^2)$ and $\Psi_2(Q^2)$ are irrelevant for the sum rule in Eq. (11). This is due to the fact that the contributions calculated from the Borel operator, in Eq. (7), vanish for any non-negative integer powers of Q^2. For the spectral function case, non-logarithmic terms vanish when analytic continuation is performed using Eq. (9). The relevant expressions for these quantities for FOPT and RGSPT can be found in Appendix B and Sec. B 2.

The OPE contributions from the dimension-four term, $\Psi_4(Q^2)$, contain both massive corrections ($\propto m_i^4$) as well as nonperturbative condensates of quarks and gluon fields. These corrections are known to $\mathcal{O}(\alpha_s^1)$ [35,47,71]. Their RG running should also be taken into account when coupling and masses are evolved with the scale. However, we use the results provided in Refs. [72,73] to form an RG invariant combination of these condensates. For the quark condensates, this relation is given by

$$\langle m_i\bar{q}_jq_j\rangle_{\text{inv}} = \langle m_i\bar{q}_jq_j\rangle + m_im_j^3\left(\frac{3}{7\pi^2x} - \frac{53}{56\pi^2}\right). \quad (34)$$

The RG invariant combinations of the condensates [72] also introduce inverse powers of the α_s [35,74]. For the gluon condensate, we use the following relation:

$$\frac{\beta(x)}{x^2}\left\langle\frac{\alpha_s}{\pi}G^2\right\rangle_{\text{inv}} \equiv \frac{\beta(x)}{x^2}\left\langle\frac{\alpha_s}{\pi}G^2\right\rangle - 4\gamma_m(x)\sum_{k=u,d,s}\langle m_i\bar{q}_iq_i\rangle$$
$$- \frac{3}{4\pi^2}\gamma_{\text{vac}}\sum_{k=u,d,s}m_k^4, \qquad (35)$$

where $\gamma_{\text{vac}} = -1 - (4x)/3 + x^2(-223/72 + 2/3\zeta(3))$ is the vacuum anomalous dimension [73]. The expression for Ψ_4 in RGSPT and FOPT are provided in Appendix B and Sec. B 3.

We also consider the dimension-six contribution to the OPE, $\Psi_6(Q^2)$, for which only condensate terms are known. These corrections can be written as

$$\Psi_6(Q^2) = \frac{(I_6)_{12}}{6},$$

where

$$(I_6)_{ij} = -3(m_i\langle\bar{q}_jq_jG\rangle + m_j\langle\bar{q}_iq_iG\rangle)$$
$$- \frac{32}{9}\pi^2 x(\langle\bar{q}_iq_i\rangle^2 + \langle\bar{q}_jq_j\rangle^2 - 9\langle\bar{q}_iq_i\rangle\langle\bar{q}_jq_j\rangle). \quad (36)$$

Subscripts i and j stand for the quark flavors in the strange and nonstrange channels. It should be noted that the structure of the dimension-six condensate is rather complicated and, in deriving Eq. (36), vacuum saturation approximation is used to relate dimension-six four-quark condensate terms to dimension-four quark condensates. For more details, we refer to [2,35].

The numerical values used for the nonperturbative quantities are as follows [75,76]:

$$\langle\bar{u}u\rangle = -\frac{f_\pi^2 M_\pi^2}{2(m_u + m_d)}, \qquad (37)$$

$$\langle\bar{s}s\rangle = (0.8 \pm 0.3)\langle\bar{s}s\rangle \quad [28], \qquad (38)$$

$$\left\langle\frac{\alpha_s}{\pi}G^2\right\rangle = 0.037 \pm 0.015 \text{ GeV}^4, \qquad (39)$$

$$\langle\bar{q}_iq_iG\rangle = M_0^2\langle\bar{q}_iq_i\rangle \quad [12], \qquad (40)$$

$$M_0^2 = 0.8 \pm 0.2 \text{ GeV}^2 \quad [12]. \qquad (41)$$

We neglect the contributions to OPE beyond this order.

From Eq. (33), we can obtain $\Psi_5''(Q^2)$, which has following form:

$$\Psi_5''(Q^2) = \frac{(m_1 + m_2)^2}{Q^2}\sum_{i=0}\frac{\tilde{\Psi}_i''(Q^2)}{(Q^2)^i}, \qquad (42)$$

and the Borel transform as

$$\Psi_5''(u) = \frac{(m_1 + m_2)^2}{u}\sum_{i=0}\frac{\tilde{\Psi}_i''(u)}{u^i}. \qquad (43)$$

The spectral function from Eq. (33) is obtained by using Eq. (9), and it can be organized as

$$\rho_5^{\text{OPE}}(s) = s\mathcal{R}_0(s) + \mathcal{R}_2(s) + \frac{1}{s}\mathcal{R}_4(s)$$
$$+ \frac{1}{s^2}\mathcal{R}_6(s) + \cdots, \qquad (44)$$

where $\mathcal{R}_n$ are calculated from Ψ_n using (46) and analytical expressions for $\mathcal{R}_0$ can be found in Ref. [28]. It should be noted that $\rho_5^{\text{OPE}}(s)$ and $\Psi_5''(Q^2)$ are RG invariant perturbative quantities that enter in the Borel-Laplace sum rule in Eq. (11).

The $\Psi_n(q^2)$ for the pseudoscalar current appearing in the OPE of Eq. (33) are not a RG invariant quantity. The Adler function $\mathcal{D}_n(Q^2)$ is obtained from it using the relation

$$\mathcal{D}_n(Q^2) \equiv -Q^2\frac{d}{dQ^2}[(m_1 + m_2)^2\Psi_n(Q^2)], \qquad (45)$$

which is RG invariant, and $m_i = m_i(Q)$ as mentioned before in the text below Eq. (4). Both $\Psi_n(Q^2)$ and $\mathcal{D}_n(Q^2)$ have a cut $Q^2 = -q^2 < 0$ due to the term $\log(\frac{\mu^2}{-q^2})$. The spectral density in Eq. (44) is obtained in the timelike regions ($s = q^2 > 0$) from the discontinuity of the polarization function,

$$\mathcal{R}_n(s) \equiv \frac{1}{2\pi i}\lim_{\epsilon\to 0}[\Psi_n(-s - i\epsilon) - \Psi_n(-s + i\epsilon)]$$
$$= \frac{1}{2\pi i}\int_{-s+i\epsilon}^{-s-i\epsilon}dq^2\frac{d}{dq^2}\Psi_n(q^2)$$
$$= \frac{-1}{2\pi i}\int_{-s+i\epsilon}^{-s-i\epsilon}\frac{dq^2}{q^2}\mathcal{D}_n(q^2)$$
$$= \frac{-1}{2\pi i}\oint_{|x_c|=1}\frac{dx_c}{x_c}\mathcal{D}_n(-x_cs). \qquad (46)$$

The contour integral in the above equation has to be evaluated without crossing the cut for $q^2 > 0$. It should be noted that for FOPT and RGSPT prescriptions, the imaginary part can be obtained trivially by replacing the $\log(\mu^2/Q^2) = \log(\mu^2/|Q|^2) \pm i\pi$ across the cut. For the numerical evaluation methods, such as in the CIPT prescriptions, Eq. (46) can be very useful for analytic continuation in the complex plane. To sum π^2-terms in RGSPT, we first perform the RG improvement of the

$\Psi_n(q^2)$ or $\mathcal{D}_n(q^2)$. The resulting perturbative has the most general term given in Eq. (19) for which the imaginary part can be taken by simply setting $\log(\mu^2/Q^2) = \log(\mu^2/|Q|^2) \pm i\pi$. This process results in an analytic expression for which the renormalization scale can be set $\mu^2 = s$, but the $i\pi$ terms are left behind, which results in improved convergence. For more details about their effects on the summation of kinematical terms, we refer to [23].

It should be noted that the analytic continuation using the RGSPT expressions for the $\mathcal{R}_n$ are rather lengthy. Therefore, we provide expressions for corresponding Adler functions in Appendix B.

A. Analytic continuation in FOPT and RGSPT

The $\mathcal{R}_i(s)$ are obtained from $\Psi_n(q^2)$ by its analytic continuation from spacelike regions to timelike regions [using Eq. (46)], which results in the large kinematical π^2 corrections. These corrections, however, can be summed to all orders using RGSPT, and a good convergence is obtained for the perturbative series. As a demonstration, we define R_0 from $\mathcal{R}_0$ as

$$R_0 \equiv \frac{8\pi^2}{3(m_s(2))^2} \mathcal{R}_0. \tag{47}$$

Using $\alpha_s(2 \text{ GeV}) = 0.2945$ and $m_s(2 \text{ GeV}) = 93.4 \text{ MeV}$ and setting $m_u = 0$, the R_0 at different orders of α_s has the following contributions:

$$R_0^{\text{FOPT}} = 1.0000 + 0.6612 + 0.4909 + 0.2912 \\ + 0.1105, \tag{48}$$

$$R_0^{\text{RGSPT}} = 1.0038 + 0.4175 + 0.1760 + 0.0581 \\ - 0.0152. \tag{49}$$

We can see that summation of the π^2-terms enhances the convergence of the perturbation series when RGSPT is employed. The scale dependence of the R_0 and truncation uncertainty at different scales are significantly improved, which can be seen in Fig. 2(a).

We can also test the RG improvement for the $\tilde{\Psi}_0''(q^2)$ by defining $\bar{\Psi}_0''(q^2)$, analogous to Eq. (47), as

$$\bar{\Psi}_0''(q^2) \equiv \frac{8\pi^2}{3(m_s(2 \text{ GeV}))^2} \tilde{\Psi}_0, \tag{50}$$

and using quark masses and α_s the same as R_0 and setting $q = 2 \text{ GeV}$, we get the following contributions to $\bar{\Psi}_0''^{,\text{FOPT}}(q^2)$:

$$\bar{\Psi}_0''^{,\text{FOPT}} = 1.0000 + 0.4737 + 0.2837 + 0.1917 \\ + 0.1405, \tag{51}$$

$$\bar{\Psi}_0''^{,\text{RGSPT}} = 1.1508 + 0.5280 + 0.2621 + 0.1670 \\ + 0.1244. \tag{52}$$

In the case of $\bar{\Psi}_0''(q^2)$, we get slightly better convergence than FOPT. The scale dependence of $\bar{\Psi}_0''(q^2)$ normalized to unity at 2 GeV is plotted in Fig. 2(b).

B. Borel transform in FOPT and RGSPT

The perturbative series in the FOPT prescription is a polynomial form containing α_s, m_q^2/Q^2, and $\log(\frac{\mu^2}{Q^2})$. For Borel transforms in FOPT, only terms $\log(\frac{\mu^2}{Q^2})$ and Q^2 are relevant, and we get an analytical expression containing Euler's constant, ζ functions in addition to terms $\log(\frac{\mu^2}{u})$, and powers of u. To obtain the Borel transform, we use the relation from Ref. [35] for the operator in Eq. (7),
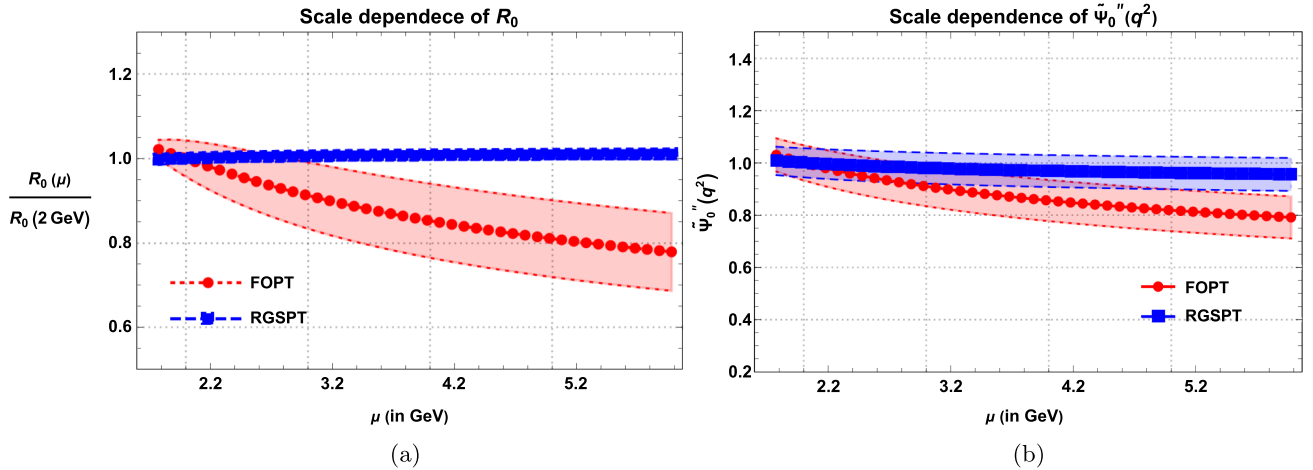
FIG. 2. Renormalization scale dependence of (a) $R_0(s)$ and (b) $\bar{\Psi}_0''(q^2)$ normalized to unity at 2 GeV in RGSPT and FOPT. The bands represent the truncation uncertainty.

$$\hat{\mathcal{B}}_u\left[\frac{1}{(Q^2)^\alpha}\log^n\left(\frac{\mu^2}{Q^2}\right)\right]$$

$$= \frac{1}{(u)^\alpha}\sum_{k=0}^{n}(-1)^{kn}C_k\log^k\left(\frac{\mu^2}{u}\right)\partial_\alpha^{n-k}\left(\frac{1}{\Gamma[\alpha]}\right), \quad (53)$$

where ${}^nC_k = \frac{n!}{k!(n-k)!}$ is the binomial coefficient. The derivative of the Γ function results in the appearance of the Euler's constant and ζ functions that can be seen in Eq. (64).

For RGSPT, Borel transform is not a trivial task; it involves a transcendental function as encountered in Ref. [77] and is evaluated numerically. The most general term in RGSPT, from Eq. (19), can be written as

$$\frac{\log^n(w)}{w^\alpha} = [\partial_\delta^n w^{\delta-\alpha}]_{\delta\to0}, \quad (54)$$

where $w = 1 - \beta_0 x\log(\mu^2/s)$ and α is some real number depending upon the anomalous dimension of the quantity under consideration.

Using Schwinger parametrization, we can write

$$\frac{1}{w^\alpha} = \frac{1}{\Gamma[\alpha]}\int_0^\infty dt\, t^{\alpha-1}e^{-tw}$$

$$= \frac{1}{\Gamma[\alpha]}\int_0^\infty dt\, t^{\alpha-1}e^{-t(1-\beta_0 x\log(\mu^2/s))}$$

$$= \frac{1}{\Gamma[\alpha]}\int_0^\infty dt\, t^{\alpha-1}(\mu^2/s)^{\beta_0 xt}e^{-t}$$

$$= \frac{1}{\Gamma[\alpha]}\sum_{n=0}^{\infty}\frac{(-1)^n}{\Gamma[n+1]}\int_0^\infty dt\, t^{\alpha+n-1}(\mu^2/s)^{\beta_0 xt}. \quad (55)$$

Using the above relation, we can easily perform the Borel operator as follows:

$$\hat{\mathcal{B}}_u\left[\frac{1}{s^z}\frac{1}{w^\alpha}\right] = \frac{1}{(\mu^2)^z\Gamma[\alpha]}\sum_{n=0}^{\infty}\frac{(-1)^n}{\Gamma[n+1]}$$

$$\times \int_0^\infty dt\frac{t^{\alpha+n-1}}{\Gamma[z+\beta_0 xt]}(\mu^2/u)^{\beta_0 xt+z}, \quad (56)$$

where we have used the identity

$$\hat{\mathcal{B}}_u\left[\frac{1}{s^\alpha}\right] = \frac{1}{\Gamma[\alpha]u^\alpha}. \quad (57)$$

Now, we rescale the integral in Eq. (56) by substituting $\tilde{t} = \beta_0 xt$ and rewrite it as

$$\hat{\mathcal{B}}_u\left[\frac{1}{s^z}\frac{1}{w^\alpha}\right] = \frac{1}{(\mu^2)^z\Gamma[\alpha]}\sum_{n=0}^{\infty}\frac{(-1)^n}{\Gamma[n+1](\beta_0 x)^{n+\alpha}}$$

$$\times \int_0^\infty d\tilde{t}\frac{\tilde{t}^{\alpha+n-1}}{\Gamma[z+\tilde{t}]}(\mu^2/u)^{\tilde{t}+z}. \quad (58)$$

We can see that integral in the above relation cannot be evaluated analytically [78]. We use

$$\tilde{\mu}(z,b,a) \equiv \int_0^\infty dt\frac{x^{a+t}t^b}{\Gamma[b+1]\Gamma[a+t+1]} \quad (59)$$

to rewrite Eq. (58) as

$$\hat{\mathcal{B}}_u\left[\frac{1}{s^z}\frac{1}{w^\alpha}\right] = \frac{1}{(\mu^2)^z\Gamma[\alpha]}\sum_{n=0}^{\infty}\frac{(-1)^n\Gamma[\alpha+n-1]}{\Gamma[n+1](\beta_0 x)^{n+\alpha}}$$

$$\times \tilde{\mu}(\mu^2/u,\alpha+n-1,z). \quad (60)$$

We have to rely on numerical methods beyond this point. However, the identity

$$\int_0^\infty e^{-st}\tilde{\mu}(t,b,a)dt = s^{-\alpha-1}(\log(s))^{-\beta-1}, \quad (61)$$

allows us to recover the original function using Laplace transform.

Now, we can demonstrate the impact of the resummation for the Borel transformation. Consider leading mass corrections at different dimension to $\tilde{\Psi}_j''(s)$ from RGSPT, which has the following form:

$$A_j^{\text{RGSPT}} = \frac{1}{s(1-\beta_0 xL)^{(2j+2)\gamma_0/\beta_0}}, \quad (62)$$

where $L = \log(\mu^2/s)$ is used here for the discussion. Its series expansion to $\mathcal{O}(\alpha_s^4)$ in FOPT is given by

$$A_j^{\text{FOPT}} = \frac{1}{s}\left(1 + 2\gamma_0 L(j+1)x + \gamma_0 L^2(j+1)x^2(\beta_0 + 2\gamma_0(1+j))\right.$$

$$+ \frac{2}{3}\gamma_0 L^3(j+1)x^3(\beta_0 + (1+j)\gamma_0)(\beta_0 + 2\gamma_0(1+j))$$

$$\left.+ \frac{1}{6}\gamma_0 L^4(j+1)x^4(\beta_0 + \gamma_0(1+j))(\beta_0 + 2\gamma_0(1+j))(3\beta_0 + 2\gamma_0(1+j))\right) + \mathcal{O}(\alpha_s^5). \quad (63)$$

Now, the Borel transformation of the above series can be obtained by substituting the following values:

$$\hat{\mathcal{B}}_u\left[\frac{1}{s}\right] = \frac{1}{u}, \qquad \hat{\mathcal{B}}_u\left[\frac{\log(\frac{\mu^2}{s})}{s}\right] = \frac{\log(\frac{\mu^2}{u}) + \gamma_E}{u},$$

$$\hat{\mathcal{B}}_u\left[\frac{\log^2(\frac{\mu^2}{s})}{s}\right] = \frac{\log^2(\frac{\mu^2}{u}) + 2\gamma_E \log(\frac{\mu^2}{u}) + \gamma_E^2 - \zeta(2)}{u},$$

$$\hat{\mathcal{B}}_u\left[\frac{\log^3(\frac{\mu^2}{s})}{s}\right] = \frac{(3\gamma_E^2 - 3\zeta(2))\log(\frac{\mu^2}{u}) + 3\gamma_E\log^2(\frac{\mu^2}{u})}{u}$$
$$+ \frac{\log^3(\frac{\mu^2}{u}) + 2\zeta(3) + \gamma_E^3 - 3\gamma_E\zeta(2)}{u},$$

$$\hat{\mathcal{B}}_u\left[\frac{\log^4(\frac{\mu^2}{s})}{s}\right] = \frac{8\gamma_E\zeta(3) + \gamma_E^4 + 3/2\zeta(4) - 6\gamma_E^2\zeta(2)}{u}$$
$$+ \frac{\log(\frac{\mu^2}{u})(8\zeta(3) + 4\gamma_E^3 - 12\gamma_E\zeta(2))}{u}$$
$$+ \frac{(6\gamma_E^2 - 6\zeta(2))\log^2(\frac{\mu^2}{u}) + \log^4(\frac{\mu^2}{u})}{u}$$
$$+ \frac{4\gamma_E\log^3(\frac{\mu^2}{u})}{u}, \tag{64}$$

where γ_E is Euler's constant, and $\zeta(i)$ are the ζ functions. These induced terms as a property of Borel-Laplace sum rules are first pointed in Ref. [79].[3] It is interesting to note that all the γ_E can be absorbed in the logarithms, i.e., $\log(\frac{\mu^2 e^{\gamma_E}}{u})$, but not the ζ functions. A similar case for the Fourier transform of the static potential from momentum to the position space can be found in Ref. [80].

Now, we obtain the Borel transform for A_0 using Eq. (64) and by setting $\mu^2 = u = 2.5$ GeV^2 that resums the logarithms in the case of FOPT. Using $x(\sqrt{2.5}) = \alpha_s(\sqrt{2.5})/\pi = 0.3361/\pi$, the Borel transformation of A_0 has the following contributions:

$$\hat{\mathcal{B}}_u[A_0^{\mathrm{RGSPT}}] = 0.4256,$$
$$\hat{\mathcal{B}}_u[A_0^{\mathrm{FOPT}}] = 0.4000 + 0.0494 - 0.0255 - 0.0011 + 0.0042$$
$$= 0.4270. \tag{65}$$

It is clear from these numerical contributions that numerical contributions from leading logarithms are oscillatory, and the Borel transformation has poor convergence. These oscillations are due to the nonlogarithmic terms of Eq. (64) [as we have set $\log(\frac{\mu^2}{u}) = 0$]. The convergence gets worse for higher j values, which can be inferred from Eq. (63), and the first three are plotted in Fig. 4. The RGSPT value is all-order

---

[3] We thank Professor Narison for bringing this reference to our attention.
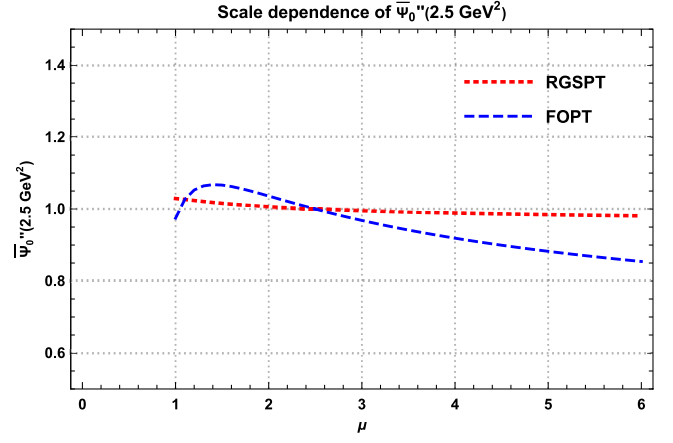
FIG. 3. Scale dependence of the $\tilde{\Psi}_0''(u)|_{u=2.5 \text{ GeV}^2}$ in RGSPT and FOPT.

results, but for FOPT, it oscillates and slowly converges to the RGSPT value.

We can use the above results to study the renormalization scale dependence of $\tilde{\Psi}_0''(u)$. To compare FOPT and RGSPT results, we use values of $\tilde{\Psi}_0''(u)|_{u=2.5 \text{ GeV}^2}$ in these prescriptions, normalized to unity at $\mu = 2.5$ GeV, and present our results in Fig. 3. Again, results for RGSPT are very stable for a wide range of renormalization scales.

C. Convergence of Borel transformed OPE using FOPT and RGSPT

We use the ratio $r_n^{d=0,2}$, defined in Ref. [28], from Eq. (43) as

$$r_n^{d=0,2}(u) = \frac{\left(\frac{1}{u}\tilde{\Psi}_0''(u) + \frac{1}{u^2}\tilde{\Psi}_2''(u)\right)^{(\mathcal{O}(\alpha_s^n))}}{\Psi''(u)}. \tag{66}$$

The numerator in the above equation is evaluated using the contributions from $\mathcal{O}(\alpha_s^n)$ from dimension-zero and dimension-two corrections to $\Psi''(u)$. Using PDG values for the $m_s(2 \text{ GeV}) = 93.4$, $m_d(2 \text{ GeV}) = 4.67$ MeV and setting $u = 2.5$ GeV^2, we get the following contributions to $r_n^{d=0,2}$:

$$r_n^{d=0,2}|_{\mathrm{FOPT}} = \{53.45\%, 27.46\%, 13.30\%, 3.51\%, -0.22\%\},$$
$$r_n^{d=0,2}|_{\mathrm{RGSPT}} = \{59.25\%, 23.52\%, 8.34\%, 4.04\%, 2.35\%\}.$$

From these numerical values, one may suspect that the FOPT has better convergence than RGSPT. This behavior can be attributed to the fact that there are large negative corrections from the Borel transform of the logarithmic $\log^n(\mu^2/Q^2)$ terms as depicted in Fig. 4. The behavior of r_n for different values of the Borel parameter can be found in Fig. 5.

These findings clearly show that RGSPT has the potential to reduce theoretical uncertainty significantly and has been the primary goal of this article.
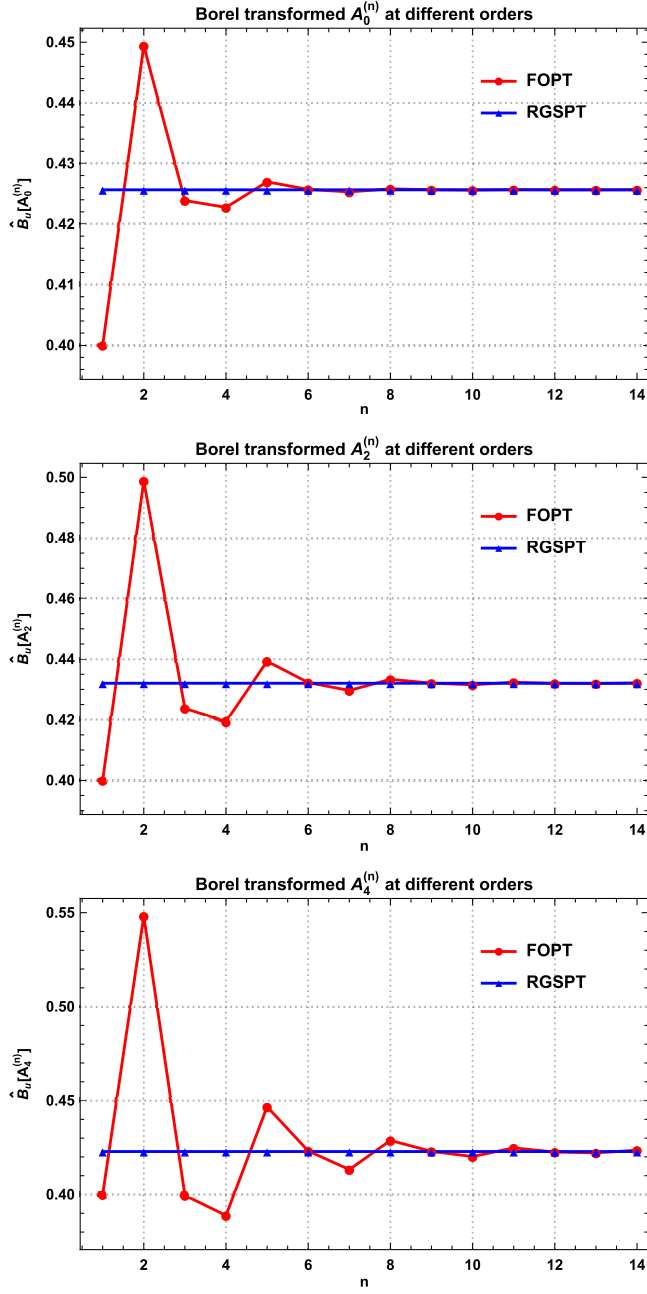
FIG. 4. A_n calculated at different orders using $\mu^2 = u = 2.5$ GeV^2.

D. Instanton contribution

In addition to the OPE correction, the QCD vacuum structure becomes relevant at low energy, and contributions from the instantons become relevant at energy range ~ 1 GeV. Their contributions are estimated using the instanton liquid model (ILM) [81–83] and are added to the pseudoscalar current correlator. These contributions are parametrized in terms of the instanton size ρ_c and number density n_c. For the spectral density, we use the results from Refs. [31,48,84],

$$\rho_{i,j}^{\text{inst}} = \frac{1}{2\pi} \text{Im}(\Psi(s)_{\text{inst}})$$

$$= \frac{-3\eta_{ij}(m_i + m_j)^2}{4\pi} J_1(\rho_c \sqrt{s}) Y_1(\rho_c \sqrt{s}), \quad (67)$$

where $\rho_c = 1/0.6$ and $\eta_{ud/us} = 1/0.6$ [83]. In addition, we also need the Borel transform of the second derivative of the polarization function for the instanton, which is given by [32]

$$\Psi_{5,ij}''(u)^{\text{inst}} = \hat{\mathcal{B}}_u[(\Psi_5''(s))_{\text{inst}}]$$

$$= \frac{3\eta_{ij}\rho_c^2(m_i + m_j)^2}{8\pi^2} e^{-\frac{1}{2}\rho_c^2 u}$$

$$\times \left[K_0\left(\frac{1}{2}\rho_c^2 u\right) + K_1\left(\frac{1}{2}\rho_c^2 u\right) \right], \quad (68)$$

where K_0 and K_1 are the modified Bessel functions. These contributions are numerically relevant for low values of the Borel parameter $u \sim 1$ GeV^2.

Now, we have all the theoretical and phenomenological quantities needed as input for the Borel sum rule in Eq. (11). In the next section, light quark mass determination using FOPT and RGSPT is performed.

VI. LIGHT QUARK MASS DETERMINATION

In this section, we determine that masses of the strange quark mass using the Borel-Laplace sum rule in Eq. (11) from the divergences of the axial vector current. It should be noted that the m_u is determined using the ratio $\epsilon_{ud} \equiv m_u/m_d = 0.474^{+0.056}_{-0.074}$ [66].

Before moving to mass determination from the Sum rule, we need to fix the values for the continuum threshold s_0 and Borel parameter u. In principle, any determination from the Borel-Laplace sum rule should be independent of the choice of these parameters in the limit $u \gg s_0$. However, in practical cases, there is a dependence on the determinations of light quark masses on these parameters. For practical purposes, these parameters are tuned to get stable results for a given range. The Borel parameter is chosen large enough to suppress the contributions from nonperturbative condensate terms and resonances. However, the continuum threshold s_0 is chosen in a region where contributions from the higher resonances are negligible and spectral function can be approximated with the continuum pQCD correction. A proper window for s_0 and u is crucial for the stable determination of the Borel-Laplace sum rule, and we have discussed them for FOPT and RGSPT and in this section for the individual as well as simultaneous m_d and m_s determination.

We can also perform quark mass determination by choosing the value of s_0 for which both hadronic and perturbative spectral functions are in agreement. However, these determinations are going to be very sensitive to the second
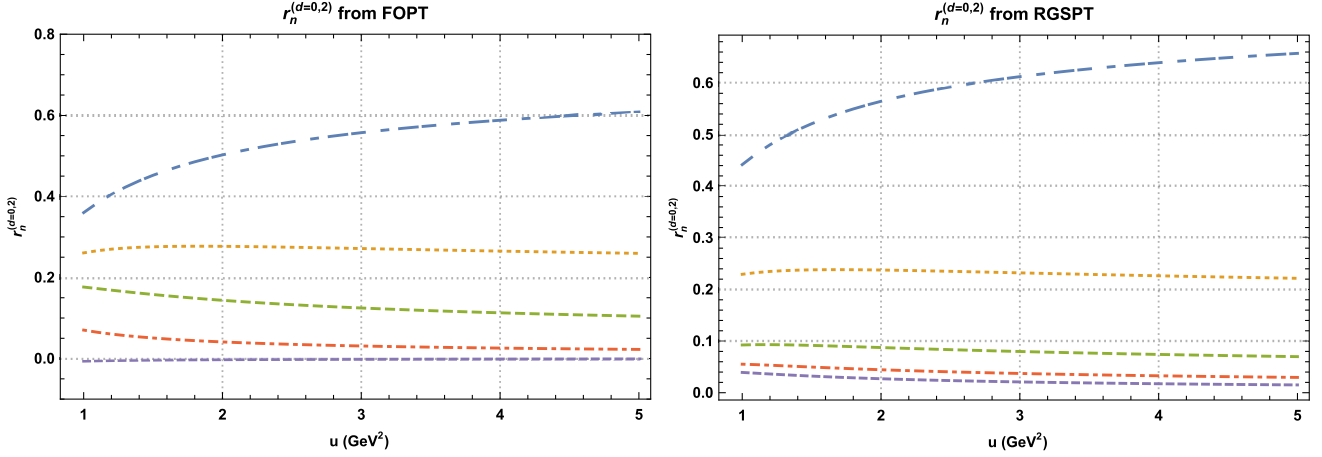
FIG. 5. $r_n^{d=0,2}$ from FOPT and RGSPT. The lines from top to bottom correspond to $n = 0, 1, 2, 3, 4$.

resonance present in the hadronic spectral function. Another issue is the absence of information about higher resonances, which are already neglected in this study. Various contributions to the spectral functions are presented in Fig. 6 for nonstrange and strange channels. For these channels, this agreement is found in the range $s_0 \in [3.38, 3.79]$, for which we have taken $s_0 = 3.58 \pm 0.20 \, \text{GeV}^2$ in such determinations. However, such determinations are not taken in our final average due to the issues discussed above.
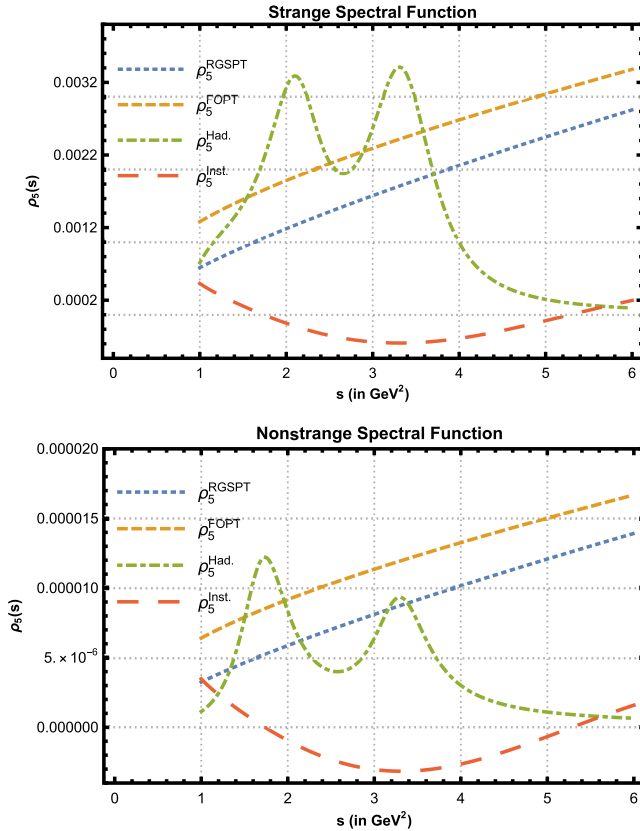
FIG. 6. Hadronic and theoretical spectral functions in the strange and nonstrange channel.

A. m_s determination

To fix the free s_0 and u parameters, we first perform m_s determination at different values. In the FOPT prescription, there is a crossover around $s_0 = 4.5 \, \text{GeV}^2$ for different values of the Borel parameter that can be seen in Fig. 10(a). Therefore, we choose $s_0 = 4.5 \pm 0.5 \, \text{GeV}^2$ to minimize variation in the m_s determination with respect to the Borel parameter from FOPT determinations. However, this is not the case for RGSPT as there is no crossing point in Fig. 10(b). There is a stability window for the $s_0 \in [3.5, 4.2] \, \text{GeV}^2$ region for RGSPT, but we do not use this value as $\sqrt{s_0}$ is close to the mass of the second resonance. This results in slightly more uncertainty from the variation of u in the m_s determination compared to FOPT, which can be seen in Fig. 10(c). However, we find that there is a linear increase in the difference of maximum and minimum values of strange quark mass $[\Delta(m_s)]$ determination for $s_0 \in [3, 5] \, \text{GeV}^2$ with $u \in [2, 3]$, which can be seen in Fig. 10(d). This linear behavior is milder in the case of RGSPT compared to FOPT.

Now, we move on to our final determination, for which we adopt the choice of parameters used in Ref. [28]. For the Borel parameter, we use $u = 2.5 \pm 0.5 \, \text{GeV}^2$ and the renormalization scale is varied in the range $u/2 \leq \mu^2 \leq 2u$. We take the continuum threshold value $s_0 = 4.5 \pm 0.5 \, \text{GeV}^2$ and $m_u = 2.16^{+0.49}_{-0.26} \, \text{MeV}$ [66] as input in our determination. We obtain the following value of $m_s(2 \, \text{GeV})$, using FOPT:

$$m_s(2 \, \text{GeV}) = 103.64^{+6.45}_{-4.61} \, \text{MeV}, \tag{69}$$

and for RGSPT, we obtain

$$m_s(2 \, \text{GeV}) = 104.20^{+4.37}_{-4.29} \, \text{MeV}. \tag{70}$$

The details of significant sources of uncertainties can be found in Table I. The pQCD uncertainties contain uncertainties arising from uncertainties present in the quark and

TABLE I. m_d and m_s determination using FOPT and RGSPT and the sources of uncertainties denoted in the column.

Quark mass	FOPT						RGSPT					
	Final value	μ	α_s	u	s_0	pQCD	Had.	Final value	μ	α_s	u	s_0	pQCD	Had.
$m_d(2\text{ GeV})$	$4.18^{+0.51}_{-0.44}$	$+0.18$ -0.07	$+0.06$ -0.06	$+0.07$ -0.05	$+0.08$ -0.09	$+0.20$ -0.11	$+0.47$ -0.43	$4.21^{+0.48}_{-0.39}$	$+0.02$ -0.01	$+0.06$ -0.06	$+0.10$ -0.08	$+0.05$ -0.07	$+0.10$ -0.10	$+0.47$ -0.38
$m_s(2\text{ GeV})$	$103.64^{+6.45}_{-4.61}$	$+4.59$ -1.66	$+1.40$ -1.40	$+0.76$ -0.52	$+2.59$ -2.66	$+5.14$ -2.85	$+3.91$ -3.62	$104.20^{+4.37}_{-4.29}$	$+0.55$ -0.52	$+1.42$ -1.40	$+1.40$ -1.48	$+1.76$ -2.13	$+2.45$ -2.43	$+3.61$ -3.54

gluon condensates, α_s, renormalization scale variation, and truncation uncertainty. The truncation uncertainty is calculated from the contribution of the last terms present in the expansion of α_s in the perturbative series. Uncertainties from other parameters are included in the hadronic uncertainties (abbreviated as Had. Tables I and II).

It is worth mentioning that the uncertainties coming from scale variation in RGSPT are significantly smaller than in FOPT, leading to small pQCD uncertainties compared to the hadronic uncertainties. It is important to note from Table I is that the total theoretical uncertainty from pQCD parameters is smaller than the hadronic uncertainties when RGSPT is used. We present the scale dependence in our determinations in Fig. 8(b). Another point to note is that the exclusion of the instanton term for the RGSPT and FOPT series leads to a decrease of strange quark mass about 1.26 and 1.24 MeV, respectively.

Now, we also present our results for the value of s_0 at which theoretical and hadronic spectral functions are in agreement. Using $s_0 = 3.58 \pm 0.20$ GeV^2 and taking the rest of the parameters discussed above, we get the following determinations for the FOPT and RGSPT schemes:

$$m_s(2\text{ GeV}) = 107.29^{+7.57}_{-5.83}\text{ MeV}\quad(\text{FOPT}),\quad(71)$$

$$m_s(2\text{ GeV}) = 106.02^{+4.36}_{-4.57}\text{ MeV}\quad(\text{RGSPT}).\quad(72)$$

The dependence of these determinations on the Borel parameter is presented in Fig. 7.

B. m_d determination

Similar to m_s determination, there is a crossover point for m_d in FOPT, but near to $\pi(1800)$ resonance mass as we can see in Fig. 9. Because of this, we choose $s_0 = 4.5 \pm 0.5$ GeV^2 as in the previous subsection. Using the same parameters and ϵ_{ud} [66] for FOPT, we obtain the following values:

$$m_d(2\text{ GeV}) = 4.18^{+0.51}_{-0.44}\text{ MeV},\quad(73)$$

$$\Rightarrow m_u(2\text{ GeV}) = 1.98^{+0.34}_{-0.37}\text{ MeV},\quad(74)$$

and for RGSPT, we obtain the following value:

$$m_d(2\text{ GeV}) = 4.21^{+0.48}_{-0.39}\text{ MeV},\quad(75)$$

$$\Rightarrow m_u(2\text{ GeV}) = 2.00^{+0.33}_{-0.36}\text{ MeV}.\quad(76)$$

We present the scale dependence in our determinations in Fig. 8(a). The details of the sources of uncertainties can be found in Table I. Exclusion of the instanton terms leads to a decrease in the central value of $m_d(2\text{ GeV})$ by 0.20 and 0.13 MeV in determinations using FOPT and RGSPT prescriptions, respectively.

Now, using $s_0 = 3.58 \pm 0.20$ GeV^2 and taking the rest of the parameters discussed above, we get the following determinations for FOPT and RGSPT schemes:

$$m_d(2\text{ GeV}) = 4.30^{+0.52}_{-0.46}\text{ MeV}\quad(\text{FOPT}),\quad(77)$$

$$\Rightarrow m_u(2\text{ GeV}) = 2.04^{+0.35}_{-0.40}\text{ MeV},\quad(78)$$

$$m_d(2\text{ GeV}) = 4.26^{+0.46}_{-0.39}\text{ MeV}\quad(\text{RGSPT}),\quad(79)$$

$$\Rightarrow m_u(2\text{ GeV}) = 2.02^{+0.32}_{-0.40}\text{ MeV}.\quad(80)$$

The dependence of these determinations on the Borel parameter can be found in Fig. 7.
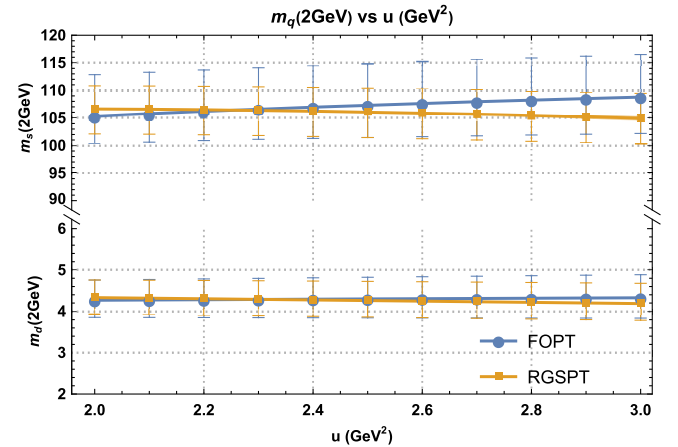
FIG. 7.   Borel parameter dependence of the individual determinations of $m_d(2\text{ GeV})$ assuming quark-hadron duality is obeyed at $s_0 =$ from FOPT and RGSPT prescriptions.
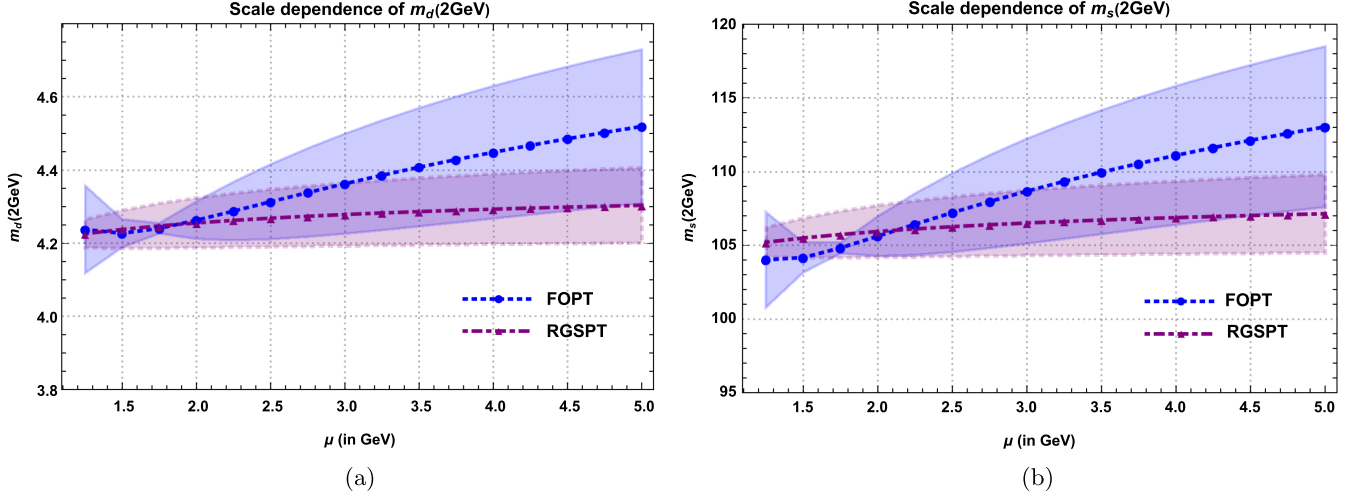
FIG. 8.   The scale dependence in the individual (a) m_d and (b) m_s determinations using FOPT and RGSPT. The bands in the plot represent truncation uncertainty at different scales.
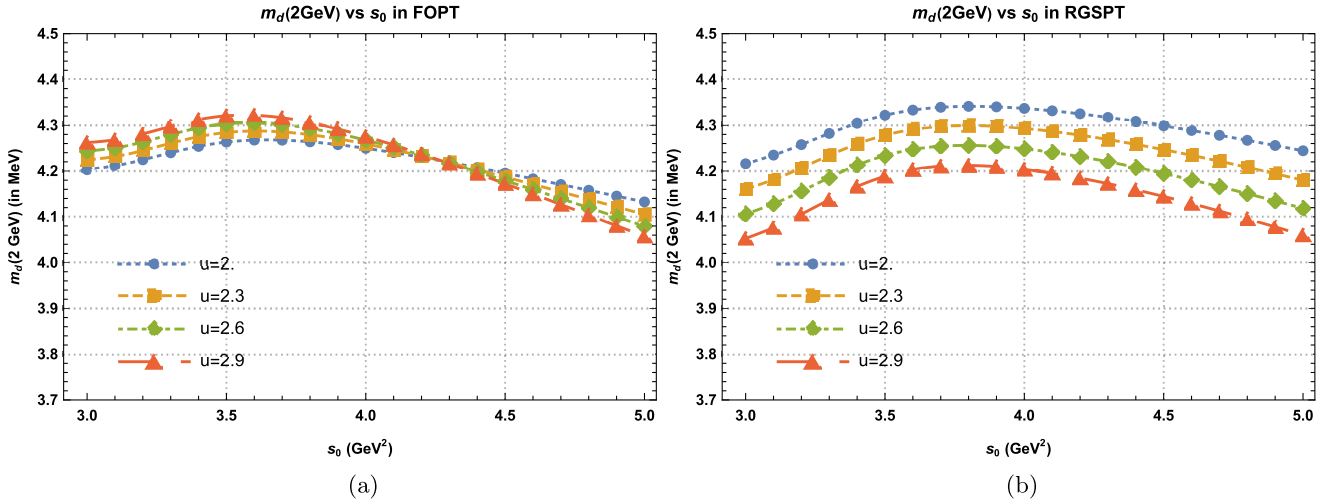
FIG. 9. $m_d(2 \text{ GeV})$ calculated at different values of Borel parameter and s_0 using (a) FOPT and (b) RGSPT prescriptions.

C. Simultaneous m_d and m_s determination

We can also perform the simultaneous determination of the m_s and m_d using the sum rule in Eq. (11) for strange and nonstrange channels. Using FOPT, we obtain

$$m_s(2 \text{ GeV}) = 103.80^{+6.14}_{-4.22} \text{ MeV}, \tag{81}$$

$$m_d(2 \text{ GeV}) = 4.18^{+0.50}_{-0.44} \text{ MeV}, \tag{82}$$

$$\Rightarrow m_u(2 \text{ GeV}) = 1.98^{+0.33}_{-0.37} \text{ MeV}, \tag{83}$$

and for RGSPT, we obtain the following values:

$$m_s(2 \text{ GeV}) = 104.34^{+4.32}_{-4.24} \text{ MeV}, \tag{84}$$

$$m_d(2 \text{ GeV}) = 4.21^{+0.48}_{-0.45} \text{ MeV}, \tag{85}$$

$$\Rightarrow m_u(2 \text{ GeV}) = 2.00^{+0.33}_{-0.38} \text{ MeV}. \tag{86}$$

The details of sources of uncertainties in the determination of quark masses can be found in Table II. In this case, uncertainty in m_s determination is smaller than the one obtained in Sec. VI A. The values obtained for m_s and m_d are very close to the determination from Secs. VI A and VI B.
Using $s_0 = 3.58 \pm 0.20 \text{ GeV}^2$ for FOPT, we obtain

$$m_s(2 \text{ GeV}) = 107.39^{+6.95}_{-5.08} \text{ MeV}, \tag{87}$$

$$m_d(2 \text{ GeV}) = 4.30^{+0.51}_{-0.44} \text{ MeV}, \tag{88}$$

$$\Rightarrow m_u(2 \text{ GeV}) = 2.04^{+0.34}_{-0.40} \text{ MeV}, \tag{89}$$

TABLE II. m_d and m_s determination using FOPT and RGSPT and the sources of uncertainties denoted in the column.

Quark mass	FOPT						RGSPT					
	Final value	μ	α_s	u	s_0	pQCD	Had.	Final value	μ	α_s	u	s_0	pQCD	Had.
$m_d(2 \text{ GeV})$	$4.18^{+0.50}_{-0.44}$	$+0.18$ -0.07	$+0.06$ -0.06	$+0.07$ -0.05	$+0.08$ -0.09	$+0.19$ -0.09	$+0.47$ -0.43	$4.21^{+0.48}_{-0.45}$	$+0.02$ -0.01	$+0.06$ -0.06	$+0.10$ -0.08	$+0.05$ -0.07	$+0.10$ -0.10	$+0.47$ -0.43
$m_s(2 \text{ GeV})$	$103.80^{+6.14}_{-4.22}$	$+4.54$ -1.66	$+1.38$ -1.38	$+0.72$ -0.49	$+2.56$ -2.62	$+4.77$ -2.24	$+3.87$ -3.58	$104.34^{+4.32}_{-4.24}$	$+0.55$ -0.52	$+1.41$ -1.38	$+1.34$ -1.44	$+1.74$ -2.11	$+2.42$ -2.40	$+3.57$ -3.50

and for RGSPT, we obtain the following values:

$$m_s(2 \text{ GeV}) = 106.14^{+4.32}_{-4.52} \text{ MeV}, \tag{90}$$

$$m_d(2 \text{ GeV}) = 4.26^{+0.46}_{-0.43} \text{ MeV}, \tag{91}$$

$$\Rightarrow m_u(2 \text{ GeV}) = 2.02^{+0.32}_{-0.40} \text{ MeV}. \tag{92}$$

VII. SUMMARY AND CONCLUSION

We have used the Borel-Laplace sum rule to determine the light quark masses from the correlator of the divergence of the axial vector current. The sum rule uses both hadronic as well as perturbative contributions. In Sec. III, we briefly reviewed the procedure of RG summation in RGSPT and its importance in the RG improvement for the theoretical quantities used in the Borel-Laplace sum rule.
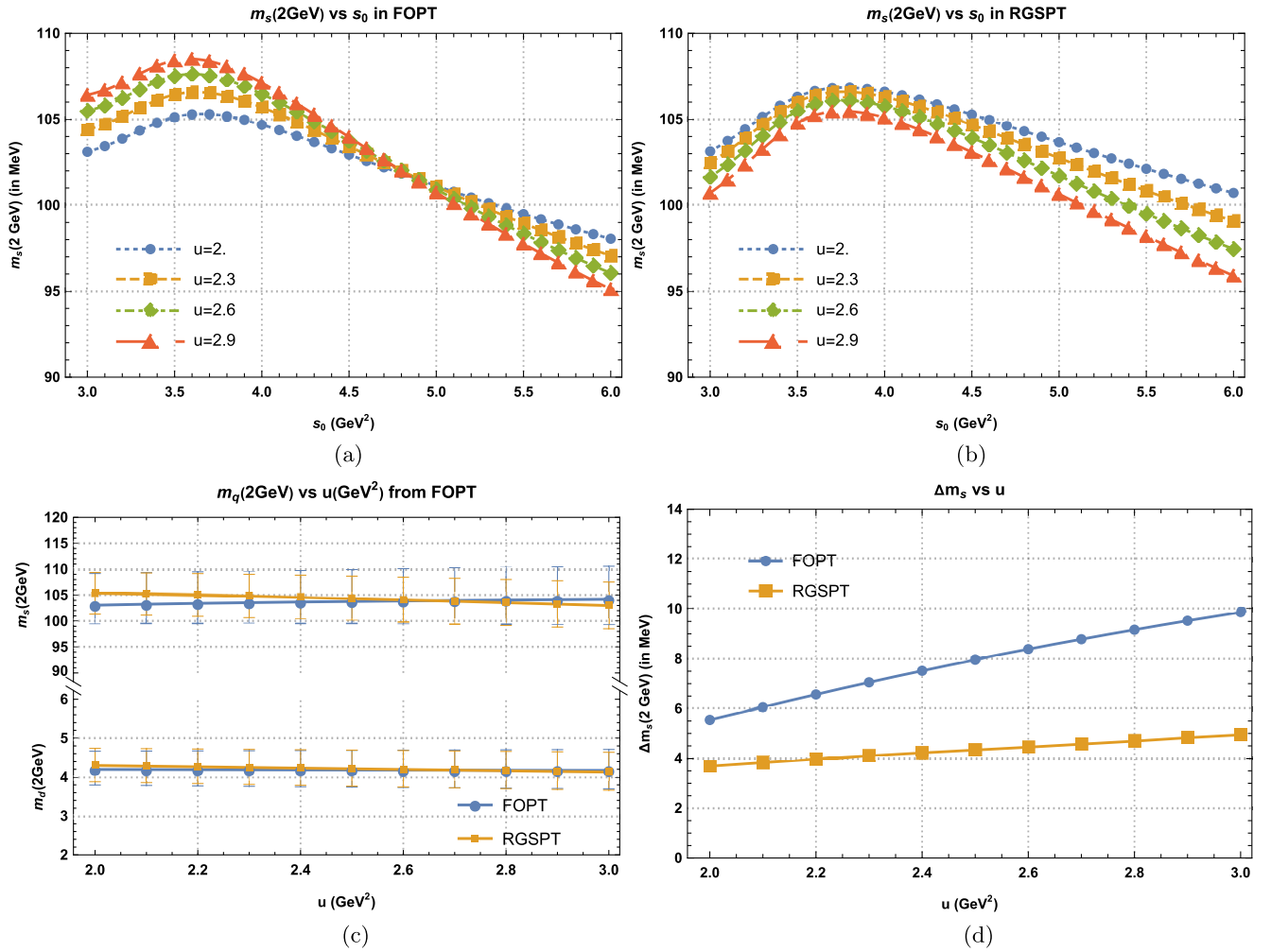
FIG. 10. $m_s(2 \text{ GeV})$ calculated at different values of Borel parameter and s_0 using (a) FOPT and (b) RGSPT schemes. In Fig. (c), $m_s(2 \text{ GeV})$ and $m_d(2 \text{ GeV})$ at different values of the Borel parameter in the range $u \in [2, 3] \text{ GeV}^2$. In (d), $\Delta m_s(2 \text{ GeV})$ obtained by varying $s_0 \in [3, 5] \text{ GeV}^2$ at different values of Borel parameter u.

In Sec. IV, we discussed the hadronic pseudoscalar spectral function for which no experimental information is available. However, these contributions can be parametrized in terms of the information available on the masses and decay width of the spectral function. We use commonly used hadronic parametrization from Dominguez and de Rafael [49] in this article for the light quark mass determination, and it has a good agreement with another parametrization by Maltman and Kambor [48], which can be seen in Fig. 1.

In Sec. V, the continuum contributions are discussed in detail. The most commonly used FOPT prescription results are already available in the literature. These determinations have large uncertainties from the variation of the renormalization scale. RGSPT can reduce such uncertainties and is inspired by the findings of Ref. [23]; we first sum the kinematical π^2-terms appearing due to analytic continuation of the spectral function in Sec. V A. The analytic continuation using RGSPT also results in better convergence of the perturbation series for the dimension-zero contribution. We also find better convergence and improved scale dependence for the $\Psi''(Q^2)$, which is also an RG invariant quantity. These improvements can be seen in Fig. 2.

In Sec. V B, we first calculated the Borel transformation for the $\Psi''(Q^2)$ in the RGSPT prescription. The Borel transformation for RGSPT can only be performed numerically, and it resums all the Euler's constant and various ζ functions that arise due to Borel transformation for RGSPT. The FOPT results are found to be poorly convergent and oscillate around the all-order result from the RGSPT. RGSPT also improves the scale dependence of the Borel transformed $\Psi''(Q^2)$ which is used as input in the Borel-Laplace sum rule in Eq. (11). These improvements can be seen in Figs. 3 and 4. The result obtained is used in Sec. V C to test the convergence of $\Psi''(u)$. The FOPT series is found to be slightly more convergent than RGSPT, but it is argued that RGSPT results are more trustworthy as Borel transformation in FOPT has oscillatory behavior for the known results. We also include small instanton contributions using results from ILM in Sec. V D.

We determined the light quark masses in Sec. VI using the free parameters s_0 and u used in Ref. [28]. This particular choice leads to small u dependence in the FOPT determinations of the m_s, which can be seen in Fig. 10(a). For the RGSPT determination, the stability region is closer to the second resonance; therefore, we have used the choices for these free parameters from FOPT. This leads to slightly large uncertainty in the m_s determination from the variations of u. In addition to the individual determination of the m_s and m_d, we have performed simultaneous determination and found a slightly more precise value for m_s. These results are presented in Tables I and II. In addition to this, we have also presented our determination by choosing $s_0 = 3.58 \pm 0.20$ GeV^2 in the resonance region where there is good agreement

between theoretical and hadronic spectral function. These values result in higher values of the quark masses which can be seen in Figs. 10(a) and 10(b). Since this value choice of s_0 is sensitive to the parameters of the second resonance and higher resonances are neglected, we do not consider them in our final determinations.

Now, we give our final determination for the light quark masses, which comes from the simultaneous determination of the m_s and m_d and their values at 2 GeV are

$$m_s(2 \text{ GeV}) = 104.34^{+4.32}_{-4.24} \text{ MeV}, \tag{93}$$

$$m_d(2 \text{ GeV}) = 4.21^{+0.48}_{-0.45} \text{ MeV}, \tag{94}$$

$$m_u(2 \text{ GeV}) = 2.00^{+0.33}_{-0.40} \text{ MeV}. \tag{95}$$

Corresponding PDG average values [66] are

$$m_s(2 \text{ GeV}) = 93.4^{+8.6}_{-3.4} \text{ MeV}, \tag{96}$$

$$m_d(2 \text{ GeV}) = 4.67^{+0.48}_{-0.17} \text{ MeV}, \tag{97}$$

$$m_u(2 \text{ GeV}) = 2.16^{+0.49}_{-0.26} \text{ MeV}, \tag{98}$$

which is in agreement with our findings.

ACKNOWLEDGMENTS

APPENDIX A: RUNNING OF THE STRONG COUPLING AND THE QUARK MASSES IN THE pQCD

The running of strong coupling and the quark masses are computed by solving the following differential equations:

$$\mu^2 \frac{d}{d\mu^2} x(\mu) = \beta(x) = -\sum_i x^{i+2} \beta_i,$$

$$\mu^2 \frac{d}{d\mu^2} m(\mu) \equiv m\gamma_m = -m \sum_i \gamma_i x^{i+1}, \tag{A1}$$

where β_i are the QCD β function coefficients and γ_i are the quark mass anomalous dimension.

The QCD β function coefficients are known to five loops [85–93] and their analytic expression for n_f-active flavor are

$$\beta_0 = \frac{11}{4} - \frac{1}{6}n_f, \qquad \beta_1 = \frac{51}{8} - \frac{19}{24}n_f, \qquad \beta_2 = \frac{2857}{128} - \frac{5033}{1152}n_f + \frac{325}{3456}n_f^2,$$

$$\beta_3 = \frac{149753}{1536} - \frac{1078361}{41472}n_f + \frac{50065}{41472}n_f^2 + \frac{1093}{186624}n_f^3 + \frac{891}{64}\zeta(3) - \frac{1627}{1728}n_f\zeta(3) + \frac{809}{2592}n_f^2\zeta(3),$$

$$\beta_4 = \frac{8157455}{16384} + \frac{621885\zeta(3)}{2048} - \frac{9801\pi^4}{20480} - \frac{144045\zeta(5)}{512} + n_f\left(-\frac{336460813}{1990656} - \frac{1202791\zeta(3)}{20736} + \frac{6787\pi^4}{110592} + \frac{1358995\zeta(5)}{27648}\right)$$

$$+ n_f^2\left(\frac{25960913}{1990656} + \frac{698531\zeta(3)}{82944} - \frac{5263\pi^4}{414720} - \frac{5965\zeta(5)}{1296}\right) + n_f^3\left(-\frac{630559}{5971968} - \frac{24361\zeta(3)}{124416} + \frac{809\pi^4}{1244160} + \frac{115\zeta(5)}{2304}\right)$$

$$+ n_f^4\left(\frac{1205}{2985984} - \frac{19\zeta(3)}{10368}\right). \tag{A2}$$

The known five-loop quark mass anomalous dimension coefficients [94–101] are

$$\gamma_m^{(0)} = 1, \qquad \gamma_m^{(1)} = \frac{1}{4^2}\left(\frac{202}{3} + \frac{-20}{9}n_f\right), \qquad \gamma_m^{(2)} = \frac{1}{4^3}\left(1249 + n_f\left(-\frac{160\zeta(3)}{3} - \frac{2216}{27}\right) - \frac{140n_f^2}{81}\right),$$

$$\gamma_m^{(3)} = \frac{1}{4^4}\left(\frac{135680\zeta(3)}{27} - 8800\zeta(5) + \frac{4603055}{162} + n_f\left(-\frac{34192\zeta(3)}{9} + 880\zeta(4) - \frac{18400\zeta(5)}{9} - \frac{91723}{27}\right)\right.$$

$$\left. + n_f^2\left(\frac{800\zeta(3)}{9} - \frac{160\zeta(4)}{3} + \frac{5242}{243}\right) + n_f^3\left(\frac{64\zeta(3)}{27} - \frac{332}{243}\right)\right),$$

$$\gamma_m^{(4)} = \frac{1}{4^5}\left(\frac{99512327}{162} + \frac{46402466\zeta(3)}{243} + 96800\zeta(3)^2 - \frac{698126\zeta(4)}{9} - \frac{231757160\zeta(5)}{243} + 242000\zeta(6) + 412720\zeta(7)\right.$$

$$+ n_f\left(-\frac{150736283}{1458} - \frac{12538016\zeta(3)}{81} - \frac{75680\zeta(3)^2}{9} + \frac{2038742\zeta(4)}{27} + \frac{49876180\zeta(5)}{243} - \frac{638000\zeta(6)}{9}\right.$$

$$\left. - \frac{1820000\zeta(7)}{27}\right) + n_f^2\left(+\frac{1320742}{729} + \frac{2010824\zeta(3)}{243} + \frac{46400\zeta(3)^2}{27} - \frac{166300\zeta(4)}{27} - \frac{264040\zeta(5)}{81} + \frac{92000\zeta(6)}{27}\right)$$

$$\left. + n_f^3\left(\frac{91865}{1458} + \frac{12848\zeta(3)}{81} + \frac{448\zeta(4)}{9} - \frac{5120\zeta(5)}{27}\right) + n_f^4\left(-\frac{260}{243} - \frac{320\zeta(3)}{243} + \frac{64\zeta(4)}{27}\right)\right). \tag{A3}$$

APPENDIX B: CONTRIBUTION TO CURRENT CORRELATOR

1. Dimension-zero contributions

The zero-dimensional contribution to OPE is known to five loops (α_s^4) [42–44]. We are using the following expression for Ψ_0:

$$\Psi_0(q^2) = \frac{3}{8\pi^2}\left\{L + \left(L^2 + \frac{17L}{3}\right)x + x^2\left(\frac{17L^3}{12} + \frac{95L^2}{6} + L\left(\frac{9631}{144} - \frac{35\zeta(3)}{2}\right)\right)\right.$$

$$+ x^3\left[L^2\left(\frac{4781}{18} - \frac{475\zeta(3)}{8}\right) + \frac{221L^4}{96} + \frac{229L^3}{6} + L\left(-\frac{91519\zeta(3)}{216} + \frac{715\zeta(5)}{12} - \frac{\pi^4}{36} + \frac{4748953}{5184}\right)\right]$$

$$+ x^4\left[L\left(\frac{192155\zeta(3)^2}{216} - \frac{46217501\zeta(3)}{5184} + \frac{455725\zeta(5)}{432} - \frac{52255\zeta(7)}{256} - \frac{125\pi^6}{9072} - \frac{3491\pi^4}{10368} + \frac{7055935615}{497664}\right)\right.$$

$$\left.\left. + L^2\left(-\frac{1166815\zeta(3)}{576} + \frac{24025\zeta(5)}{96} - \frac{\pi^4}{36} + \frac{97804997}{20736}\right) + L^3\left(\frac{3008729}{3456} - \frac{5595\zeta(3)}{32}\right) + \frac{51269L^4}{576} + \frac{1547L^5}{384}\right]\right\}, \tag{B1}$$

where $x \equiv \alpha_s(\mu)/\pi$ and $L = \log(\frac{\mu^2}{-q^2})$. This expression reproduces the results for $\mathcal{R}_0$ and $\tilde{\Psi}_0''(u)$ in Ref. [28].

For RGSPT, these quantities can be derived using Eqs. (45) and (46) from the Adler function. The RGSPT expression for the dimension-zero Adler function is given by

$$\mathcal{D}_0(q^2) = \frac{3(m_i + m_j)^2}{8\pi^2 w^{\frac{8}{9}}} \left\{ 1 + x\left(-1.790 + \frac{7.457}{w} - \frac{1.580 \log(w)}{w}\right) + x^2\left(-0.339 + \frac{60.699}{w^2} + \frac{2.653 \log^2(w)}{w^2} - \frac{14.514}{w}\right.\right.$$

$$+ \left.\left(\frac{2.829}{w} - \frac{27.849}{w^2}\right)\log(w)\right) + x^3\left(-\frac{129.189}{w^2} + \frac{599.649}{w^3} - \frac{4.542 \log^3(w)}{w^3} + \left(\frac{76.231}{w^3} - \frac{4.750}{w^2}\right)\log^2(w)\right.$$

$$+ \left.\left(\frac{53.766}{w^2} - \frac{361.248}{w^3} + \frac{0.536}{w}\right)\log(w) - \frac{5.207}{w} + 0.593\right) + x^4\left(-12.673 + \frac{15.012}{w} - \frac{66.312}{w^2} - \frac{1339.755}{w^3}\right.$$

$$+ \frac{6992.440}{w^4} + \frac{7.851 \log^4(w)}{w^4} + \left(\frac{8.131}{w^3} - \frac{183.752}{w^4}\right)\log^3(w) + \left(-\frac{146.509}{w^3} + \frac{1384.280}{w^4} - \frac{0.901}{w^2}\right)\log^2(w)$$

$$+ \left.\left.\left(\frac{18.438}{w^2} + \frac{759.073}{w^3} - \frac{4787.937}{w^4} - \frac{0.938}{w}\right)\log(w)\right)\right\}, \tag{B2}$$

where $w = 1 - x(\mu)\beta_0 \log(\frac{\mu^2}{-q^2})$.

2. Dimension-two corrections

The dimension-two contributions with full mass dependence are available to $\mathcal{O}(\alpha_s^1)$ in Refs. [35,45–47]. Additional $\mathcal{O}(\alpha_s^2)$ correction is taken from Ref. [28]. For FOPT, we use the following expression for dimension-two contribution to the current correlator:

$$\Psi_2 = \frac{3}{8\pi^2}\left\{(m_i^2 + m_j^2)\left(x^2\left(-\frac{25L^3}{3} - \frac{97L^2}{2} + L\left(\frac{154\zeta(3)}{3} - \frac{5065}{36}\right)\right) + \left(-4L^2 - \frac{32L}{3}\right)x - 2L\right)\right.$$

$$- \left.m_i m_j\left(x\left(-4L^2 - \frac{56L}{3} + 8\zeta(3) - \frac{88}{3}\right) - 2L - 4\right)\right\}. \tag{B3}$$

For RGSPT, we derive the spectral function from the dimension-two Adler function,

$$\mathcal{D}_2 = \frac{(m_i + m_j)^2(m_i^2 + m_j^2)}{139968\pi^2 w^{34/9}}(8x(729(20w^2 - 251)x\zeta(3) + 32\log(w)(8w(290x - 81) + 1600x\log(w) - 12607x))$$

$$+ 52488w^2 + (5497360 - w(7643w + 1797332))x^2 + 1296(361 - 145w)wx)$$

$$+ \frac{(m_i + m_j)^2 m_i m_j}{216\pi^2 w^{25/9}}(w(290x - 81) + 256x\log(w) - 1046x). \tag{B4}$$

3. Dimension-four contributions

The dimension-four contributions can be obtained from Refs. [35,47,71]. For dimension-four contributions, we use an RG invariant combination of the condensates given in Refs. [72,73]. The constant terms at this order are important for the Borel-Laplace operator. We give a summed expression for the current correlator,

$$\Psi_4 = -\frac{1}{162w^{17/9}}(w(145x - 81) + 128x\log(w) - 442x)\left\langle\sum_{i=u,d,s}\bar{q}_i q_i\right\rangle_{\text{inv}} + \frac{2x}{9w^{17/9}}(\langle\bar{q}_d q_d + \bar{q}_u q_d\rangle_{\text{inv}}$$

$$+ \frac{\langle\bar{q}_i q_j + \bar{q}_j q_j\rangle_{\text{inv.}}}{81w^{17/9}}(w(145x - 81) + 128x\log(w) - 523x) - \frac{\langle\frac{\alpha_s}{\pi}G^2\rangle_{\text{inv}}}{1296w^{17/9}}(2w(145x - 81) + 256x\log(w) - 1181x)$$

$$+ \frac{1}{1512\pi^2 w^{11/3}x}\left\{(m_i^4 + m_j^4)(-324w^2 - 189wx) + m_i^2 m_j^2(x^2(-6090(w - 1) - 5376\log(w)) + 1134wx)\right.$$

$$+ (m_i^3 m_j + m_i m_j^3)(x(-3480w^2 + 5073w - 3072w\log(w)) + 648w^2 + x^2(-8555w - 7552\log(w) + 1877)))$$

$$- \left.81wx\sum_{k=u,d,s}m_k^4\right\}. \tag{B5}$$

The corresponding FOPT expression is given by

$$\Psi_4 = \frac{1}{6}((6L+11)x+3)\left\langle \sum_{i=u,d,s} \bar{q}_i q_i \right\rangle_{\text{inv}} - \frac{1}{3}(2(3L+7)x+3)(\langle \bar{q}_i q_j + \bar{q}_j q_j \rangle_{\text{inv}}) + \frac{1}{9}2x\langle \bar{q}_d q_d + \bar{q}_u q_d \rangle_{\text{inv}}$$

$$+ \frac{1}{16}\left\langle \frac{\alpha_s}{\pi} G^2 \right\rangle_{\text{inv}}((4L+11)x+2) - \frac{1}{56\pi^2 x}\left(3x \sum_{k=u,d,s} m_k^4 - m_i^3 m_j((90L+59)x+24) - m_i m_j^3((90L+59)x+24) \right.$$

$$\left. - 42xm_i^2 m_j^2 + m_i^4((45L+7)x+12) + m_j^4(45Lx+7x+12) \right). \tag{B6}$$

[1] Y. Aoki *et al.* (Flavour Lattice Averaging Group (FLAG)), Eur. Phys. J. C **82**, 869 (2022).

[2] M. A. Shifman, A. I. Vainshtein, and V. I. Zakharov, Nucl. Phys. **B147**, 385 (1979).

[3] M. A. Shifman, A. I. Vainshtein, and V. I. Zakharov, Nucl. Phys. **B147**, 448 (1979).

[4] E. C. Poggio, H. R. Quinn, and S. Weinberg, Phys. Rev. D **13**, 1958 (1976).

[5] S. Weinberg, Physica (Amsterdam) **96A**, 327 (1979).

[6] J. Gasser and H. Leutwyler, Ann. Phys. (N.Y.) **158**, 142 (1984).

[7] J. Gasser and H. Leutwyler, Nucl. Phys. **B250**, 465 (1985).

[8] S. Scherer, Adv. Nucl. Phys. **27**, 277 (2003).

[9] S. Scherer and M. R. Schindler, Lect. Notes Phys. **830**, 65 (2012).

[10] B. Ananthanarayan, M. S. A. A. Khan, and D. Wyler, Indian J. Phys. **97**, 3245 (2023).

[11] K. G. Wilson, Phys. Rev. **179**, 1499 (1969).

[12] B. L. Ioffe, Prog. Part. Nucl. Phys. **56**, 232 (2006).

[13] G. Abbas, B. Ananthanarayan, and I. Caprini, Phys. Rev. D **85**, 094018 (2012).

[14] B. Ananthanarayan and D. Das, Phys. Rev. D **94**, 116014 (2016).

[15] B. Ananthanarayan, D. Das, and M. S. A. Alam Khan, Phys. Rev. D **106**, 114036 (2022).

[16] M. R. Ahmady, F. A. Chishtie, V. Elias, A. H. Fariborz, N. Fattahi, D. G. C. McKeon, T. N. Sherry, and T. G. Steele, Phys. Rev. D **66**, 014010 (2002).

[17] M. R. Ahmady, F. A. Chishtie, V. Elias, A. H. Fariborz, D. G. C. McKeon, T. N. Sherry, A. Squires, and T. G. Steele, Phys. Rev. D **67**, 034017 (2003).

[18] B. Ananthanarayan, D. Das, and M. S. A. Alam Khan, Phys. Rev. D **102**, 076008 (2020).

[19] T. Ahmed, G. Das, M. C. Kumar, N. Rana, and V. Ravindran, arXiv:1505.07422.

[20] G. Abbas, A. Jain, V. Singh, and N. Singh, arXiv:2205.06061.

[21] M. S. A. Alam Khan, arXiv:2306.10323.

[22] F. A. Chishtie, D. G. C. Mckeon, and T. N. Sherry, Mod. Phys. Lett. A **34**, 1950047 (2019).

[23] M. S. A. Alam Khan, Phys. Rev. D **108**, 014028 (2023).

[24] D. G. C. McKeon, Int. J. Theor. Phys. **37**, 817 (1998).

[25] G. Abbas, B. Ananthanarayan, I. Caprini, and J. Fischer, Phys. Rev. D **88**, 034026 (2013).

[26] I. Caprini, J. Fischer, G. Abbas, and B. Ananthanarayan, arXiv:1711.04445.

[27] C. A. Dominguez, N. F. Nasrallah, R. Rontsch, and K. Schilcher, J. High Energy Phys. 05 (2008) 020.

[28] K. G. Chetyrkin and A. Khodjamirian, Eur. Phys. J. C **46**, 721 (2006).

[29] C. A. Dominguez, L. Pirovano, and K. Schilcher, Phys. Lett. B **425**, 193 (1998).

[30] M. Jamin, J. A. Oller, and A. Pich, Eur. Phys. J. C **24**, 237 (2002).

[31] F. H. Yin, W. Y. Tian, L. Tang, and Z. H. Guo, Eur. Phys. J. C **81**, 818 (2021).

[32] S. Narison, Phys. Lett. B **738**, 346 (2014).

[33] J. M. Yuan, Z. F. Zhang, T. G. Steele, H. Y. Jin, and Z. R. Huang, Phys. Rev. D **96**, 014034 (2017).

[34] M. Jamin, J. A. Oller, and A. Pich, Phys. Rev. D **74**, 074009 (2006).

[35] M. Jamin and M. Munz, Z. Phys. C **66**, 633 (1995).

[36] S. Narison, Nucl. Part. Phys. Proc. **270–272**, 143 (2016).

[37] Z. G. Wang, Eur. Phys. J. C **75**, 427 (2015).

[38] S. Narison, Int. J. Mod. Phys. A **30**, 1550116 (2015).

[39] P. Gelhausen, A. Khodjamirian, A. A. Pivovarov, and D. Rosenthal, Phys. Rev. D **88**, 014015 (2013); **89**, 099901(E) (2014); **91**, 099901(E) (2015).

[40] C. A. Dominguez, Int. J. Mod. Phys. A **29**, 1430069 (2014).

[41] C. A. Dominguez, N. F. Nasrallah, R. H. Rontsch, and K. Schilcher, Phys. Rev. D **79**, 014009 (2009).

[42] K. G. Chetyrkin, Phys. Lett. B **390**, 309 (1997).

[43] S. G. Gorishnii, A. L. Kataev, S. A. Larin, and L. R. Surguladze, Mod. Phys. Lett. A **05**, 2703 (1990).

[44] P. A. Baikov, K. G. Chetyrkin, and J. H. Kuhn, Phys. Rev. Lett. **96**, 012003 (2006).

[45] K. G. Chetyrkin, V. P. Spiridonov, and S. G. Gorishnii, Phys. Lett. **160B**, 149 (1985).

[46] S. C. Generalis, J. Phys. G **16**, 785 (1990).

[47] M. Jamin and M. Munz, Z. Phys. C **60**, 569 (1993).

[48] K. Maltman and J. Kambor, Phys. Rev. D **65**, 074013 (2002).

[49] C. A. Dominguez and E. de Rafael, Ann. Phys. (N.Y.) **174**, 372 (1987).

[50] J. Bijnens, J. Prades, and E. de Rafael, Phys. Lett. B **348**, 226 (1995).

[51] K. Schilcher, Mod. Phys. Lett. A **28**, 1360016 (2013).

[52] E. Braaten, S. Narison, and A. Pich, Nucl. Phys. **B373**, 581 (1992).

[53] A. A. Pivovarov, Sov. J. Nucl. Phys. **54**, 676 (1991).

[54] J. Kambor and K. Maltman, Phys. Rev. D **62**, 093023 (2000).

[55] K. Maltman and C. E. Wolfe, Phys. Lett. B **650**, 27 (2007).

[56] R. J. Hudspith, R. Lewis, K. Maltman, and J. Zanotti, Phys. Lett. B **781**, 206 (2018).

[57] D. Boito, M. Golterman, K. Maltman, S. Peris, M. V. Rodrigues, and W. Schaaf, Phys. Rev. D **103**, 034028 (2021).

[58] A. H. Hoang and C. Regner, Eur. Phys. J. Special Topics **230**, 2625 (2021).

[59] A. H. Hoang and C. Regner, SciPost Phys. Proc. **7**, 005 (2022).

[60] M. A. Benitez-Rathgeb, D. Boito, A. H. Hoang, and M. Jamin, arXiv:2111.09614.

[61] M. A. Benitez-Rathgeb, D. Boito, A. H. Hoang, and M. Jamin, J. High Energy Phys. 07 (2022) 016.

[62] M. A. Benitez-Rathgeb, D. Boito, A. H. Hoang, and M. Jamin, J. High Energy Phys. 09 (2022) 223.

[63] N. G. Gracia, A. H. Hoang, and V. Mateu, Phys. Rev. D **108**, 034013 (2023).

[64] M. Golterman, K. Maltman, and S. Peris, Phys. Rev. D **108**, 014007 (2023).

[65] C. A. Dominguez, A. Mes, and K. Schilcher, J. High Energy Phys. 02 (2019) 057.

[66] R. L. Workman *et al.* (Particle Data Group), Prog. Theor. Exp. Phys. **2022**, 083C01 (2022).

[67] A. H. Hoang, C. Lepenik, and V. Mateu, Comput. Phys. Commun. **270**, 108145 (2022).

[68] K. G. Chetyrkin, J. H. Kuhn, and M. Steinhauser, Comput. Phys. Commun. **133**, 43 (2000).

[69] F. Herren and M. Steinhauser, Comput. Phys. Commun. **224**, 333 (2018).

[70] H. Pagels and A. Zepeda, Phys. Rev. D **5**, 3262 (1972).

[71] P. Pascual and E. de Rafael, Z. Phys. C **12**, 127 (1982).

[72] V. P. Spiridonov and K. G. Chetyrkin, Sov. J. Nucl. Phys. **47**, 522 (1988).

[73] P. A. Baikov and K. G. Chetyrkin, Proc. Sci. RAD-COR2017 (**2018**) 025.

[74] K. G. Chetyrkin, C. A. Dominguez, D. Pirjol, and K. Schilcher, Phys. Rev. D **51**, 5090 (1995).

[75] M. Gell-Mann, R. J. Oakes, and B. Renner, Phys. Rev. **175**, 2195 (1968).

[76] C. A. Dominguez, L. A. Hernandez, and K. Schilcher, J. High Energy Phys. 07 (**2015**) 110.

[77] E. de Rafael, Report No. CPT-81/P-1344, https://inspirehep.net/literature/169613.

[78] A. Erdelyi, *Higher Transcendental Functions III* (Krieger Publishing Company, Malabar, FL, 1981).

[79] S. Narison and E. de Rafael, Phys. Lett. **103B**, 57 (1981).

[80] M. Jezabek, M. Peter, and Y. Sumino, Phys. Lett. B **428**, 352 (1998).

[81] E. M. Ilgenfritz and M. Muller-Preussker, Nucl. Phys. **B184**, 443 (1981).

[82] E. V. Shuryak, Nucl. Phys. **B203**, 93 (1982).

[83] E. V. Shuryak, Nucl. Phys. **B203**, 116 (1982).

[84] V. Elias, F. Shi, and T. G. Steele, J. Phys. G **24**, 267 (1998).

[85] D. J. Gross and F. Wilczek, Phys. Rev. Lett. **30**, 1343 (1973).

[86] W. E. Caswell, Phys. Rev. Lett. **33**, 244 (1974).

[87] D. R. T. Jones, Nucl. Phys. **B75**, 531 (1974).

[88] O. V. Tarasov, A. A. Vladimirov, and A. Y. Zharkov, Phys. Lett. **93B**, 429 (1980).

[89] S. A. Larin and J. A. M. Vermaseren, Phys. Lett. B **303**, 334 (1993).

[90] T. van Ritbergen, J. A. M. Vermaseren, and S. A. Larin, Phys. Lett. B **400**, 379 (1997).

[91] M. Czakon, Nucl. Phys. **B710**, 485 (2005).

[92] P. A. Baikov, K. G. Chetyrkin, and J. H. Kühn, Phys. Rev. Lett. **118**, 082002 (2017).

[93] F. Herzog, B. Ruijl, T. Ueda, J. Vermaseren, and A. Vogt, J. High Energy Phys. 02 (**2017**) 090.

[94] T. Luthe, A. Maier, P. Marquard, and Y. Schröder, J. High Energy Phys. 01 (2017) 081.

[95] R. Tarrach, Nucl. Phys. **B183**, 384 (1981).

[96] O. V. Tarasov, Phys. Part. Nucl. Lett. **17**, 109 (2020).

[97] S. A. Larin, Phys. Lett. B **303**, 113 (1993).

[98] J. A. M. Vermaseren, S. A. Larin, and T. van Ritbergen, Phys. Lett. B **405**, 327 (1997).

[99] K. G. Chetyrkin, Phys. Lett. B **404**, 161 (1997).

[100] P. A. Baikov, K. G. Chetyrkin, and J. H. Kühn, J. High Energy Phys. 10 (2014) 076.

[101] T. Luthe, A. Maier, P. Marquard, and Y. Schröder, J. High Energy Phys. 07 (2016) 127.